Heat Transfer

WILEY

HEAT TRANSFER

ORIGINAL ARTICLE

Impact of Plasma-Activated Water Pretreatment and Hot-Air Drying on Bioactive Compounds, Drying Kinetics, Structural Characteristics, and Functional Properties of Debittered Sweet Orange Peel Powder

Venkatraman Bansode[1,2] | S. Ganga Kishore[2] | Rahul Rajkumar[3] | Madhuresh Dwivedi[2] | Rama Chandra Pradhan[2] | Robbarts Nongmaithem[4] | G. Jeevarathinam[5] | Deepa Jaganathan[6]

[1]Division of Post Harvest Technology, ICAR - Central Citrus Research Institute, Nagpur, Maharashtra, India | [2]Department of Food Process Engineering, National Institute of Technology, Rourkela, Odisha, India | [3]Department of Food Technology, Dhanalakshmi Srinivasan College of Engineering, Coimbatore, Tamil Nadu, India | [4]Department of Food Technology, The Assam Royal Global University, Guwahati, Assam, India | [5]Department of Food Technology, Hindusthan College of Engineering and Technology, Coimbatore, Tamil Nadu, India | [6]Department of Food Technology, Nehru Institute of Technology, Coimbatore, Tamil Nadu, India

Correspondence: Madhuresh Dwivedi (madhureshd@gmail.com) | Rama Chandra Pradhan (pradhanrc@nitrkl.ac.in)

Received: 15 April 2025 | **Revised:** 25 August 2025 | **Accepted:** 27 August 2025

Keywords: drying kinetics | flavonoids | plasma-activated water | relative crystallinity | sweet orange | total phenols | water absorption capacity

ABSTRACT

Sweet orange peel, a major by-product of juice processing, is recognized as a bioactive-rich material abundant in phenolic compounds, offering substantial potential for valorization and sustainable by-product utilization. This study investigates the effect of plasma-activated water (PAW) pretreatment combined with hot-air tray drying on the drying behavior and quality attributes of debittered sweet orange peel. Drying was conducted under varying temperatures (50°C, 60°C, and 70°C) and air velocities (0.3, 0.6, and 0.9 m/s). The results demonstrated a significant reduction in drying time, from 465 to 225 min in treated samples (PAW-pretreated tray-dried) and from 420 to 165 min in control samples (non-pretreated tray-dried), as the temperature increased from 50°C to 70°C. Among the tested mathematical models, the logarithmic model provided the best fit for describing drying kinetics. The optimal drying condition, identified as 60°C and 0.9 m/s air velocity, resulted in sweet orange peel powder with enhanced phenolic content and improved functional, structural, and physical attributes. Treated samples exhibited significantly reduced oil absorption capacity, water absorption capacity, and swelling capacity compared with control samples. Scanning electron microscopy analysis revealed compact, dense structures in control samples, while treated samples displayed porous structures with visible spacing between particles. Relative crystallinity increased from 18.09% in control samples to 21.45% in treated samples, indicating structural transformation. Fourier-transform infrared spectroscopy confirmed the presence of key functional groups, such as hydroxyl and carbonyl, associated with the peel's bioactive compounds. These findings highlight the synergistic effect of PAW pretreatment and hot-air drying in enhancing the quality and properties of sweet orange peel powder, offering an effective strategy for the valorization of citrus fruit waste.

Practical Applications

Sweet orange peel is a rich source of bioactive substances and phenolic compounds, possessing significant health-promoting properties. Despite its potential, the high moisture content of the peel accelerates spoilage, making its preservation challenging. Utilizing drying techniques can address waste management issues while enhancing the nutritional and functional value of the product. Hot-air tray drying is an effective method for maximizing the polyphenol retention while preserving the structural, functional, morphological, and physical integrity of the peel, thereby enabling the valorization of sweet orange peel waste into nutritionally enriched products. This approach not only promotes sustainable practices but also unlocks the potential of citrus processing waste for broader industrial applications.

1 | Introduction

The sweet orange fruit (*Citrus sinensis*) belongs to the family Rutaceae and holds immense global significance due to its delicious taste, attractive flavor, and nutritious profile [1]. As per Food and Agriculture Organization, global production of sweet oranges for the 2022–2023 period was estimated at approximately 49 million metric tons. The major producing countries included Brazil, the United States, China, India, Spain, and Mexico [2]. It accounts for over 50% of global citrus production with steady annual increase in consumption, growing at an approximate rate of 3.5% over the past three decades [3]. As one of the leading cultivated citrus species, it is extensively utilized in various forms, including whole consumption and juice processing. The processing of citrus fruits for juice production results in significant waste, with approximately 50% of the fresh fruit weight ending up as seeds, pomace, and peel. This waste is often discarded into the environment [4, 5].

Discarding huge amounts of citrus waste in landfills or through incineration results in environmental pollution and can impact human health due to the release of pathogenic microbes into the air. Additionally, the mismanagement of this valuable bioresource leads to financial losses [6, 7]. Citrus waste is a valuable source of nutraceutical properties, as it has phenolic compounds, flavonoids, antioxidants, and dietary fibers [8]. These compounds derived from citrus waste hold immense potential for transformation into functional foods, food additives, pharmaceuticals, and cosmetic products. Additionally, the high carbohydrate content in fruit waste makes it an excellent substrate to produce bioethanol and biogas, offering sustainable solutions for energy generation and waste utilization [9, 10]. Citrus peel serves as an abundant source of phytochemicals, comprising vitamins, coumarins, and flavonoids found naturally in plant material [11, 12]. Thus, it is vital to investigate innovative methods for processing and utilizing orange peel to minimize resource wastage and environmental pollution. The presence of bitter compounds such as naringin and limonin in citrus peel limits its direct applicability in food products intended for human consumption. To overcome this limitation, various debittering treatments, which include salt, alkali, and solvent-based methods, have been employed to reduce the concentration of these undesirable compounds. Among the solvents tested, acetone has shown the highest efficacy in significantly decreasing the levels of naringin and limonin [13].

Plasma-activated water (PAW) pretreatment, coupled with debittering, transforms sweet orange peel waste into functional materials. PAW is produced by plasma interacting with water, generating reactive oxygen species (ROS) and reactive nitrogen species (RNS). These reactive particles drive chemical modifications in the water, enhancing its efficacy in preserving bioactive compounds and improving peel properties [14]. Drying is one of the traditional food preservation methods, enhancing the storage life of biomaterials by decreasing their moisture content. This reduction in moisture helps minimize microbial growth and enzymatic activity, thereby preserving the food for longer periods [15]. The hot-air tray drying method employs hot air at a constant or variable flow rate and temperature to remove moisture from biomaterials. This technique involves circulating warm air around the material on trays, effectively reducing its moisture content [16]. The selection of a suitable drying technique is crucial in effectively preserving bioactive compounds. Selection of a hot-air-drying method based on various factors involves the type of the product, cost of the instrument, desirable properties, energy consumption, and so forth.

A few researchers have studied the drying kinetics and modeling, as well as the effect of various drying temperatures on phenolic content, antioxidant activities, and physicochemical properties of citrus peel. Deng et al. [17] studied drying kinetics of orange peel using hot-air drying with varying temperatures and found that the Weibull model effectively represented the drying kinetics. Additionally, the quality attributes of the dried orange peel remained constant as drying time reduced from 150 to 75 min, despite a rise in temperature from 50°C to 70°C. Özcan et al. [18] reported that there was a significant increase in total phenols and flavonoid content, along with a slight reduction in antioxidant capacity and fatty acids, during the drying process of orange and lemon powder. Various drying methods, including convective, microwave, conductive, hydro, and freeze-drying, enhance levels of volatiles and phenolic compounds in the dried powders of lemon, grapefruit, orange, and bitter orange [19]. Similarly, orange peel was dried using convective, microwave, and freeze-drying methods. Among these, freeze-drying enhanced the total phenolics and antioxidant activity. The page and approximation models were observed to be the best fit in the kinetic study [20]. The maximum bioactive compounds retention was achieved at 50°C and 60°C during oven drying of pomelo peels [21]. Therefore, controlled drying processes are crucial to preserve the polyphenolic, nutritional, physical, and structural characteristics of sweet orange peel. The selection and optimization of drying methods for PAW-treated debittered sweet orange fruit peel pose significant challenges.

Currently, no studies exist on the drying process of PAW-pretreated debittered citrus fruit peel, emphasizing the necessity for further investigation. This underscores the need for further research to develop appropriate drying protocols that preserve the beneficial characteristics of the peel while ensuring efficient moisture removal and quality retention. This study aimed to

investigate the drying kinetics and modeling, as well as the effect of drying on phenolic compounds, antioxidant activities, physical properties, functional properties, and structural characteristics of PAW-treated debittered sweet orange peel powder (PDSOPP). The findings from this study are intended to offer insights for the industrial production of high-quality sweet orange peel powder to develop functional food products.

2 | Materials and Methods

2.1 | Materials

The sweet orange variety *Mosambi* was procured from the Central Citrus Research Institute in Nagpur, India. After procurement, the fruits were washed and kept at 8°C before being used in experiments. Later, the peel was subjected to PAW treatment under optimized conditions (13 kV, 62 min). These treatment conditions were established through preliminary optimization trials involving 13 different combinations of voltage and soaking durations. The selected parameters were found to yield maximal polyphenol retention and minimal antinutritional factors, and were thus employed in the present study [22]. The peel sample used for the PAW treatment was cut into uniform dimensions of 3 mm × 3 mm × 4 mm (length × width × thickness). The ratio of PAW to peel was maintained at 5:1 (w/v) during the treatment process. The PAW-treated peel was then taken for debittering treatments with a 1:10 (sample:salt) ratio. A 10% (w/v) sodium chloride (NaCl) solution was employed for the debittering treatment of the peel. The samples were immersed in the solution for 3 h at 25°C without continuous mechanical agitation. Instead, manual agitation was performed at 30-min intervals throughout the treatment period to ensure uniform exposure. The resulting PAW-treated and debittered peel was taken for drying to make peel powder under different conditions (temperature and air velocity). The control for each treatment was taken as raw sweet orange (variety *Mosambi*) peel (without any treatment). The details of treatments are mentioned in Table 1.

2.2 | Drying Experiments

Sweet orange peel was dried in a hot-air tray dryer at three different air temperatures, T_{air} (50°C, 60°C, and 70°C), and three different velocities, V_{air} (0.3, 0.6, and 0.9 m/s) to optimize the drying efficiency, preserving the quality, and controlling the properties. Further, their impact was studied on drying rate (*Rd*), moisture (*X*), and moisture ratio (*MR*). A sample of 350 g of sweet orange peel, with 4.036 ± 1.00 mm thickness, was uniformly spread on an aluminum tray in a single layer and kept in a dryer chamber. The moisture loss of sweet orange peel was recorded at a regular interval of 15 min on a digital balance. The final moisture content of sweet orange peel was determined by drying the sample at $105°C \pm 2°C$ for 24 h in a hot-air oven. The dried sweet orange peels were ground using a hammer mill (Indosaw model, India) and subsequently sieved through a 200-μm mesh to obtain a uniform powder. The resulting finely ground peel powder was used for further experimental investigations.

TABLE 1 | Drying conditions of plasma-activated water-treated and untreated samples.

PAW-treated samples	Temperature (°C)	Air velocity (m/s)	Untreated samples
DE_1	50	0.3	DE_1C
DE_2		0.6	DE_2C
DE_3		0.9	DE_3C
DE_4	60	0.3	DE_4C
DE_5		0.6	DE_5C
DE_6		0.9	DE_6C
DE_7	70	0.3	DE_7C
DE_8		0.6	DE_8C
DE_9		0.9	DE_9C

Note: DE_1, DE_2, DE_3: Treated samples at 50°C temperature and 0.3, 0.6, and 0.9 m/s air velocity.
DE_1C, DE_2C, DE_3C: Samples at 50°C temperature and 0.3, 0.6, and 0.9 m/s air velocity.
DE_4, DE_5, DE_6: Treated samples at 60°C temperature and 0.3, 0.6, and 0.9 m/s air velocity.
DE_4C, DE_5C, DE_6C: Samples at 60°C temperature and 0.3, 0.6, and 0.9 m/s air velocity.
DE_7, DE_8, DE_9: Treated samples at 70°C temperature and 0.3, 0.6, and 0.9 m/s air velocity.
DE_7C, DE_8C, DE_9C: Samples at 70°C temperature and 0.3, 0.6, and 0.9 m/s air velocity.
Abbreviation: PAW, plasma-activated water.

2.3 | Drying Characteristics

2.3.1 | Moisture Ratio and Drying Rate

The moisture ratio (*MR*) of sweet orange peel was estimated using Equation (1) as reported by Ju et al. [23]. Drying rate (*DR*) denotes the rate of moisture loss per unit time. It was determined using Equation (2) as mentioned by Bai et al. [24].

$$MR = \frac{M_t - M_e}{M_0 - M_e}, \tag{1}$$

where M_0, M_t, and M_e indicate the moisture content (g/g dry basis) at time 0, time *t*, and equilibrium, respectively.

$$DR = \frac{M_{t_1} - M_{t_2}}{t_2 - t_1}, \tag{2}$$

where t_1 and t_2 are the drying time (h); M_{t_1} and M_{t_2} indicate the moisture content (g/g dry basis) at time t_1 and t_2, respectively.

2.3.2 | Effective Moisture Diffusivity (D_{eff})

The D_{eff} was determined using Fick's second law when the drying rate curve is plotted for the sample. Equation (3) describes the relation between D_{eff} and moisture ratio (*MR*) as given by Deng et al. [25]:

$$MR = \frac{8}{\pi^2}\sum_{n=1}^{\infty}\frac{1}{n^2}e^{\left(-\frac{\pi^2 D_{\text{eff}}}{H^2}t\right)}. \quad (3)$$

Equation (3), under extended drying durations with $n = 1$, can be denoted as Equation (4).

$$MR = \frac{8}{\pi^2}e^{\left(-\frac{\pi^2 D_{\text{eff}}}{H^2}t\right)}. \quad (4)$$

Equation (5) represents the logarithmic transformation of Equation (4), where k is the slope obtained through linear regression of time curves versus ln MR. D_{eff} can then be calculated using Equation (6):

$$\ln(MR) = \ln\frac{8}{\pi^2} - \frac{\pi^2 D_{\text{eff}}}{H^2}t, \quad (5)$$

$$D_{\text{eff}} = -\frac{H^2}{\pi^2}k, \quad (6)$$

where D_{eff} denotes the effective moisture diffusivity (m^2/s), t denotes the drying time (s), and H denotes the thickness of peel (m).

2.3.3 | Activation Energy (E_a)

The temperature dependence of moisture diffusivity is described by an Arrhenius-type equation (Equation 7) as reported by Bai et al. [24] and Xie et al. [26]:

$$D_{\text{eff}} = D_0 e^{\left(-\frac{E_a}{R(T+273.15)}\right)}, \quad (7)$$

where D_0 denotes the pre-exponential factor (m^2/s), R represents the gas constant (8.314 J/mol·K), E_a represents the activation energy in kJ/mol, and T denotes the drying temperature in °C.

Equation (7) can be transformed into Equation (8) by taking the logarithm on both sides. Consequently, the activation energy (E_a) is estimated from the slope of the plot of ln(D_{eff}) versus $1/(T + 273.15)$.

$$\ln(D_{\text{eff}}) = \ln(D_0) - \frac{E_a}{R}\frac{1}{T + 273.15}. \quad (8)$$

2.4 | Kinetic Modeling

Modeling drying kinetics is valuable for predicting and optimizing the drying process. The drying model was fitted to obtained results, and the fitting was evaluated using a lower correlation coefficient (R^2), chi-square parameter (χ^2), and residual sum of squares (RSS) among experimental as well as predicted values. These evaluation metrics are expressed in Equations (9)–(11).

$$R^2 = 1 - \frac{\sum_{i=1}^{N}(A_{\text{pri},i} - A_{\text{exp},i})^2}{\sum_{i=1}^{N}(A_{\text{pri},i} - A_{\text{exp},i})^2}, \quad (9)$$

$$\chi^2 = \sum_{i=1}^{N}\frac{(A_{\text{pri},i} - A_{\text{exp},i})^2}{N - z}, \quad (10)$$

$$RSS = \sum_{i=1}^{N}(A_{\text{pri},i} - A_{\text{exp},i})^2, \quad (11)$$

where A_{pre} and A_{exp} represent the predicted and experimental values, respectively; z denotes the model parameters, and N represents the number of data.

2.5 | Total Phenolic, Flavonoid Content, and Ferric Reducing Antioxidant Power (FRAP)

Total flavonoid content in PDSOPP was assessed using the colorimetric method, and total phenol content in PDSOPP was quantified following the Folin–Ciocalteu procedure as reported by Bansode et al. [13]. The FRAP assay of PDSOPP was conducted following the procedure outlined by Bansode et al. [13].

2.6 | 2,2-Diphenyl-1-Picrylhydrazyl (DPPH)

The DPPH activity was determined using the procedure suggested by Padhi and Dwivedi [27]. The scavenging activity of the PDSOPP sample was determined using Equation (12):

$$DPPH\ \ (\%) = \left(\frac{a_0 - a_1}{a_0}\right) \times 100, \quad (12)$$

where a_0 and a_1 represent the absorbance of the control and sample mixture measured at 517 nm.

2.7 | Physical Characteristics of PDSOPP

2.7.1 | Hausner Ratio (HR) and Carr Index (CRI)

The HR ratio was determined by dividing the tapped density by the bulk density. The CRI, also known as the compressibility index, was estimated following the procedure mentioned by Bhusari et al. [28]:

$$Hausner\ \ ratio = \frac{Tapped\ \ density}{bulk\ \ density}, \quad (13)$$

$$Carr's\ \ index\ \ (\%) = \frac{Tapped\ \ density - bulk\ \ density}{tapped\ \ density} \times 100. \quad (14)$$

2.7.2 | Bulk and Tapped Density

PDSOPP was added to the 100 mL measuring cylinder until it reached the 100 mL mark, and the weight was recorded to estimate the bulk density (g/cc). To calculate the tapped density (g/cc), the cylinder was tapped 50 times on a wooden bench, and the final volume was measured. The bulk and tapped density were calculated as per the procedure suggested by Smita et al. [29].

$$Bulk\ \ density = \frac{Weight\ \ of\ \ PDSOPP}{Bulk\ \ powdered\ \ volume}, \quad (15)$$

$$Tapped\ \ density = \frac{Weight\ \ of\ \ PDSOPP}{Tapped\ \ powdered\ \ volume}. \quad (16)$$

2.7.3 | Color

The color of the flour was assessed using a Hunter Lab Colorimeter (Color Flex EZ, Hunter Lab, Virginia, USA). Calibration was performed with black and white glass standards. The color parameters measured were L^*, which ranges from 0 (black) to 100 (white); a^*, indicating redness (negative values) to greenness (positive values); and b^*, representing blueness (negative values) to yellowness (positive values). The chroma value (ΔC) is calculated by using the following equation (17):

$$\Delta C = \sqrt{a^2 + b^2}. \quad (17)$$

2.8 | Functional Properties

The functional properties of PDSOPP, including water absorption capacity (WAC) (g/g), swelling capacity (SC) (g/g), solubility index (SI) (g/g), and oil absorption capacity (OAC) (g/g), were measured following the procedure mentioned by Jaddu et al. [30].

2.9 | Structural Characteristics of PDSOPP

2.9.1 | Fourier-Transform Infrared (FTIR) Spectrometry

The FTIR spectra of PDSOPP were obtained using FTIR spectroscopy (Bruker, Alpha E FTIR, Germany). The spectra were determined at wavelength ranges from 600 to 4000/cm with 32 scans per sample [31].

2.9.2 | X-Ray Diffraction (XRD) Analysis

The XRD diffraction patterns of PDSOPP were analyzed using an X-ray diffractometer (AXSD8 Advance with Davinci Design, Bruker, Germany). The instrument was operated at 40 kV and 40 mA, with a scanning range of 2θ from 2° to 50° and a scan rate of 4°/min. The crystallinity index (CI) was calculated using Equation (18) as mentioned by Kishore et al. [31].

$$Crystallinity\ \ index\ \ (\%) = \frac{C_{PA}}{C_{PA} + A_A} \times 100, \quad (18)$$

where A_A and C_{PA} represent the amorphous area and crystalline peak area, respectively.

2.9.3 | Scanning Electron Microscopy (SEM) Analysis

The micrographs of the PDSOPP were obtained using SEM (JEOL JSM-6480 LV, Japan). The imaging conditions included an accelerated voltage of 20 kV, a magnification of ×1000, and a particle size of 10 μm [32].

2.10 | Statistical Analysis

The obtained results were analyzed utilizing SPSS software (SPSS Inc., version 21.0, USA). Duncan's multiple range test was employed to determine statistical differences between the means, with a significance level at $p < 0.05$. For model fitting, the reduced correlation coefficient (R^2), chi-square parameter (χ^2), and residual sum of squares (RSS) were utilized.

3 | Results and Discussion

3.1 | Drying Curves

Figure 1A–I illustrates the impact of various temperatures and air velocities on the drying curves of PDSOPP. The obtained results underscore the relationship between drying conditions and the overall drying time as well as the drying rate of the material. It contributes valuable knowledge to the optimization of drying processes for simple organic materials. The data clearly shows that both temperature and air velocity play crucial roles in accelerating the drying process. An increase in drying temperature (from 50°C to 70°C) combined with higher air velocity (0.3–0.9 m/s) consistently resulted in a faster reduction of moisture content [33]. The initial moisture content of treated sweet orange peel was 80.2% (w.b.), whereas the untreated peel exhibited a moisture content of 73.5% (w.b.). The overall drying times for the final moisture content (10% w.b.) ranged from 465 min at 50°C and 0.3 m/s to 225 min at 70°C and 0.9 m/s. It is evident that higher temperatures (70°C), coupled with increased air velocity (0.9 m/s), accelerated the drying rate and reduced the overall drying time. The study by Talens et al. [34] similarly reported a drying time of 120 min for orange peel at 55°C under hot-air-drying conditions. The acceleration of drying time in response to higher temperatures and air velocities can be attributed to the increased thermal energy supplied to the material and enhanced convective heat transfer. The water molecules within the PDSOPP are more readily vaporized at elevated temperatures, which reduces the time required for the drying process [35].

It is evident from the data that as drying temperature increased, the initial drying rate also increased, indicating faster moisture removal at the beginning of the drying process. This is attributed to enhanced vapor pressure and moisture diffusivity at higher temperatures, which accelerate the transfer of water from the material to the drying air. However, over time, a decline in the drying rate was observed, which can be attributed to case-hardening. Case-hardening occurs when the outer layer of the material becomes hardened due to the excessive heat. It forms a barrier that impedes more moisture transfer from the inner layers to the surface. Consequently, even though the drying conditions are more aggressive (increased temperature and air velocity), the moisture transfer rate slows down as the outer layer hardens, limiting further drying efficiency [36]. The hardening factor hinders the increase in drying rate despite

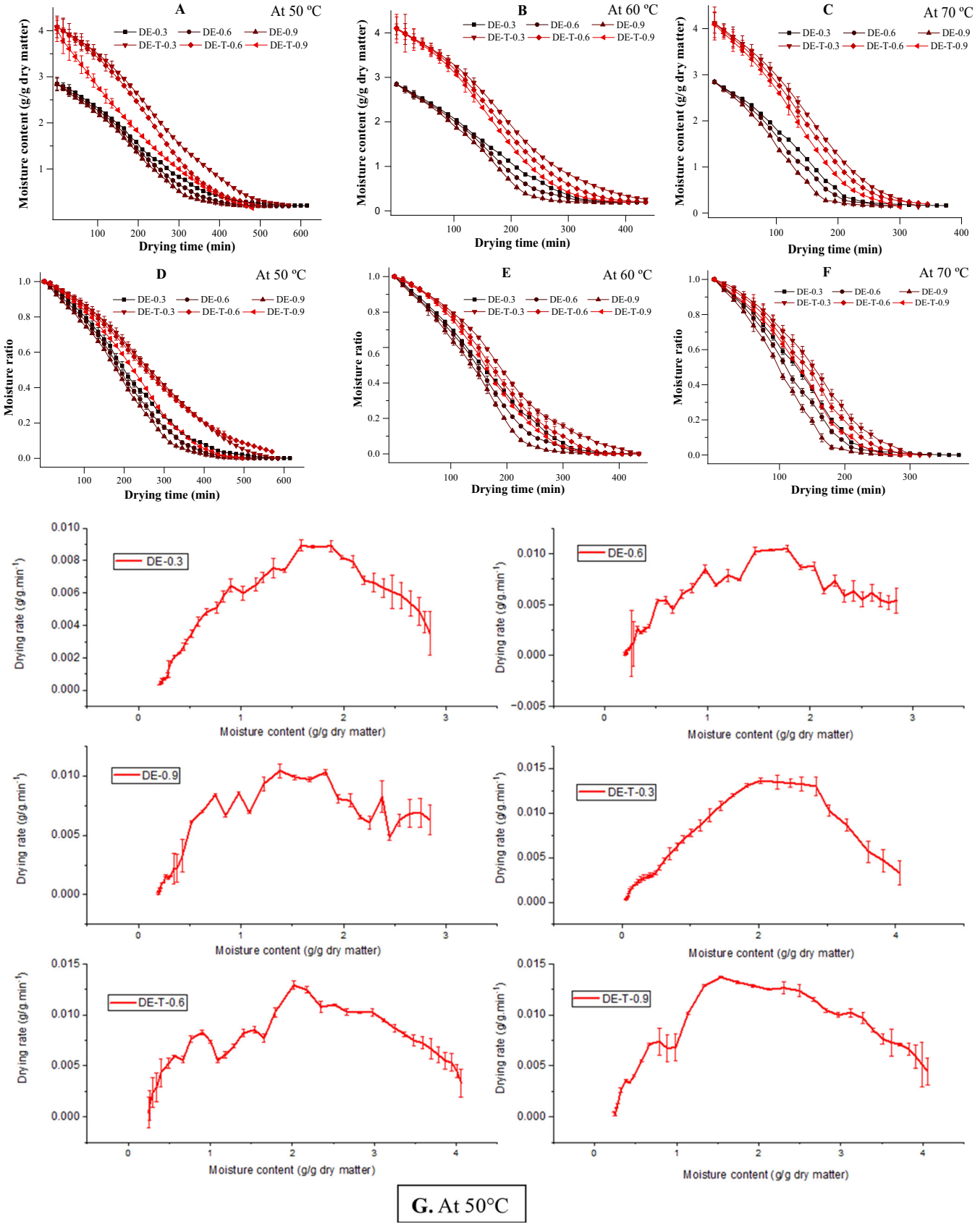

FIGURE 1 | (A–C) Moisture content versus drying time, (D–F) moisture ratio versus drying time, and (G–I) drying rate versus moisture content plots of sweet orange peel samples dried at different drying temperatures and air velocities. *Note:* DE-0.3, DE-0.6, DE-0.9—control samples; DE-T-0.3, DE-T-0.6, DE-T-0.9—treated samples.

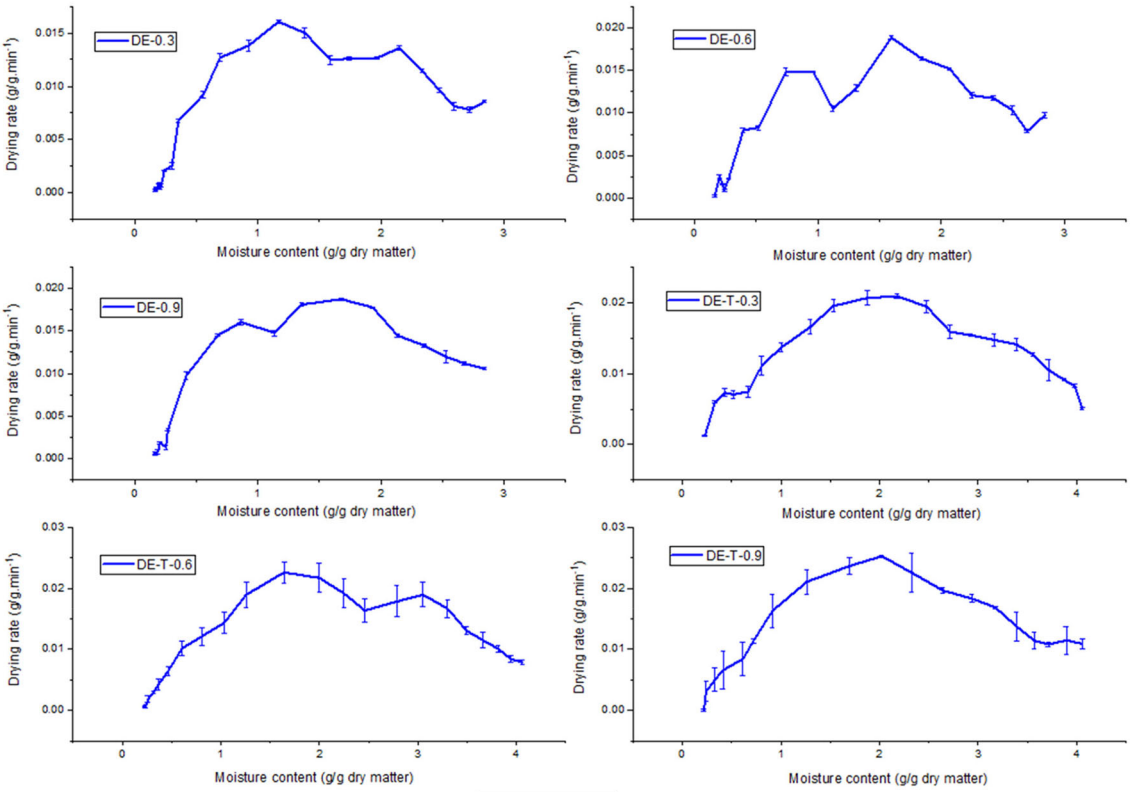

H. At 60°C

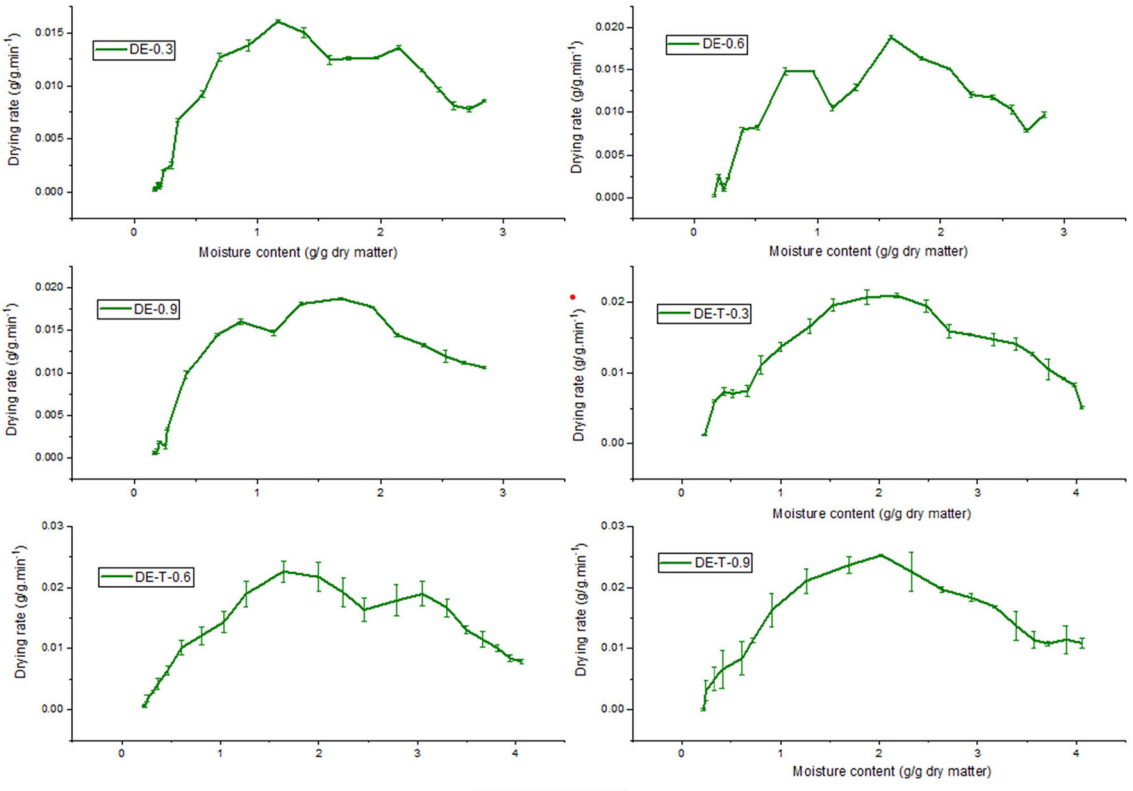

I. At 70°C

FIGURE 1 | (Continued)

increasing temperature. The obtained results corroborate previous findings from studies on case-hardening in various materials, including fruits and vegetables. The outer layer acts as a barrier to moisture diffusion during the drying process, thus reducing the rate of drying at advanced stages [37]. The finding also lines up with the study of cold plasma treatment on tobacco leaf midribs during natural drying. The use of cold plasma treatment before drying was shown to significantly reduce drying times by enhancing the moisture removal capacity. Similarly, in this study, the reduction in drying time with increasing temperature and air velocity could be seen as a form of pretreatment to the PDSOPP. The initial stages of drying are accelerated, yet the process slows as case-hardening occurs [38].

The data demonstrate a clear correlation between drying temperature, air velocity, and drying time. It is important to consider that the drying time required for PDSOPP to reach its final moisture content remains substantial even under the highest temperature and air velocity conditions. This suggests that elevated temperatures and air velocities improve drying efficiency. There may be other factors at play, such as intrinsic properties of PDSOPP, which also influence the drying kinetics. Further investigations into these factors, as well as the potential effects of pretreatment methods such as cold plasma or chemical additives, could provide additional insights [39]. In conclusion, the results highlight a significant effect of air velocity and temperature on drying kinetics, with higher ranges leading to faster drying time. It also contributes to a decline in drying rate due to case-hardening. The findings emphasize the need for a balanced approach when selecting drying parameters to avoid diminishing returns as the drying process progresses [40]. Further studies could explore the application of alternate drying techniques or pretreatment methods to further optimize the process to ultimately improve the efficiency and quality of the final product.

3.2 | Drying Kinetic Models

The analyzed models presented in Table 2 offer a comparative evaluation of the fitted models for both control and treated PDSOPP samples under different flow rates and temperatures. The comparison based on the moisture ratio and drying time experimental data utilizing three thin-layer drying models (logarithmic model, combined two-term exponential model, and page model) with drying constants was determined through nonlinear regression analysis [33]. The evaluation of model suitability was conducted by assessing key statistical parameters, which include the coefficient of determination (R^2), residual sum of squares (RSS), and the chi-squared (χ^2) values, all of which provide insight into the quality of model fit [41, 42]. The results indicate that for both control and treated PDSOPP, the logarithmic model demonstrated the best fit, as evidenced by the highest R^2 value (0.9994), alongside the lowest RSS and χ^2 values (4.811×10^{-42} and 4.681×10^{-67}, respectively). These results suggest that the logarithmic model accurately describes the drying behavior of PDSOPP under the experimental conditions studied. It indicates that the drying process primarily follows a nonlinear pattern. The excellent fit of the logarithmic model reflects its capacity to capture the dynamics of moisture removal as a function of time, especially as drying approaches its equilibrium moisture content [43]. Further details of all models can be found in Supporting Information Tables S1–S3.

It is consistent with previous studies in drying kinetics, where the logarithmic model has been found to perform well in describing moisture loss during the drying of various agricultural products, including fruits and vegetables. In particular, the model's ability to represent the slowing down of the drying rate as moisture content decreases is an important characteristic [43]. It reflects the inherent nature of moisture migration within porous materials like PDSOPP. In contrast, while other models such as the combined two-term model and the page model also showed good fits, the logarithmic model clearly outperformed them in terms of statistical accuracy. The other models useful in certain contexts may not have captured the moisture dynamics as effectively under the experimental conditions applied here [44]. This highlights the importance of model selection in drying studies, where the choice of the best-fitting model directly influences the reliability and applicability of the results [41]. The Weibull model, which was previously identified as a better fit for orange peel drying kinetics in hot-air impingement drying [34], did not emerge as the most suitable model for PDSOPP in this study. This discrepancy may be attributed to differences in the material properties of orange peel versus PDSOPP, or to the specific conditions under which the drying experiments were conducted. The Weibull model is typically favored for capturing the variability in drying rates due to its flexibility. It might not have fully captured the drying behavior of PDSOPP under the applied temperature and air velocity conditions. It suggests that material characteristics, such as pore structure, surface area, and moisture diffusivity, play a critical role in determining the appropriate model [45].

The detailed comparison of these models further emphasizes the importance of considering both the physical properties of the material being dried and the specific drying conditions in selecting an appropriate drying model. Although the logarithmic model provided the best fit in this case, future studies could explore the performance of alternative models under a broader range of conditions, as well as incorporating other factors [46]. In conclusion, the results of this model comparison confirm the suitability of the logarithmic model for accurately describing the drying kinetics of PDSOPP under the studied conditions. The consistent superiority of this model in terms of R^2, RSS, and χ^2 values suggests that it should be the model of choice for further investigations of PDSOPP drying behavior. However, continued exploration of other models, especially in relation to different drying techniques or material types, is essential for refining the understanding of drying kinetics and optimizing the drying process for various agricultural products [45, 46].

3.3 | Effective Moisture Diffusivity

The results summarized in Table 3 provide important insights into the effective diffusivity (D_{eff}) of PDSOPP under varying drying conditions. The effective diffusivity is a key parameter that governs the rate at which moisture is transferred within the

TABLE 2 | Model constants and statistical results obtained from different thin-layer drying models for control and PAW-treated samples.

	Control			PAW-treated		
Air flow (m/s)	**0.3**	**0.6**	**0.9**	**0.3**	**0.6**	**0.9**
Drying temperature: 50°C						
Logarithmic model						
a	0.1061	0.0792	0.0726	0.0694	0.1237	0.0481
b	1.0969	1.0505	0.0151	1.0523	1.1230	1.0212
k	0.0119	0.0139	0.0150	0.0104	0.0090	0.0163
R^2	0.9994	0.9991	0.9981	0.9976	0.9998	0.9983
χ^2	7.10×10^{-5}	1.14×10^{-4}	2.43×10^{-4}	2.99×10^{-4}	1.64×10^{-5}	2.28×10^{-4}
RSS	0.00277	0.00397	0.00777	0.01107	5.92×10^{-4}	0.00706
Combined two-term exponential model						
a	0.4879	0.4803	0.4752	0.4869	0.4902	0.4831
b	0.4879	0.4802	0.4745	0.4867	0.4902	0.4835
k	2.96×10^{-5}	1.78×10^{-5}	1.77×10^{-5}	7.23×10^{-6}	2.48×10^{-5}	7.23×10^{-6}
h	2.96×10^{-5}	1.78×10^{-5}	1.77×10^{-5}	7.23×10^{-6}	2.48×10^{-5}	7.23×10^{-6}
n	1.8919	2.0094	2.0315	2.0547	1.8453	2.2181
R^2	0.9992	0.9987	0.9973	0.9974	0.9995	0.9978
χ^2	9.80×10^{-5}	1.82×10^{-4}	3.66×10^{-4}	3.33×10^{-4}	5.60×10^{-5}	3.12×10^{-4}
RSS	0.00363	0.006	0.01098	0.01167	0.00190	0.00904
Page model						
n	1.8076	1.8315	1.8567	1.7727	1.9531	2.0713
k	4.30×10^{-5}	4.86×10^{-5}	5.57×10^{-5}	1.03×10^{-5}	1.35×10^{-5}	3.87×10^{-5}
R^2	0.9986	0.9970	0.9946	0.9961	0.9990	0.9959
χ^2	1.64×10^{-4}	3.74×10^{-4}	6.85×10^{-4}	4.68×10^{-4}	1.09×10^{-4}	5.29×10^{-4}
RSS	0.00655	0.01348	0.0226	0.0178	0.00403	0.01692
Drying temperature: 60°C						
Logarithmic model						
a	0.0897	0.0664	0.0519	0.0640	0.0551	0.0438
b	1.0577	1.0262	1.0022	1.0525	1.0468	1.0270
k	0.0163	0.0193	0.0223	0.0153	0.0174	0.0198
R^2	0.9976	0.9982	0.9956	0.9991	0.9992	0.9991
χ^2	3.18×10^{-4}	2.43×10^{-4}	6.29×10^{-4}	1.12×10^{-4}	1.07×10^{-4}	1.21×10^{-4}
RSS	0.00826	0.00608	0.01384			
Combined two-term exponential model						
a	0.4794	0.4760	0.4737	0.4865	0.4903	0.4867
b	0.4867	0.4902	0.4835	0.4859	0.4895	0.4868
k	7.23×10^{-6}	2.48×10^{-5}	4.36×10^{-6}	9.07×10^{-6}	8.88×10^{-6}	5.92×10^{-6}
h	7.23×10^{-6}	2.48×10^{-5}	4.36×10^{-6}	9.07×10^{-6}	8.88×10^{-6}	5.92×10^{-6}
n	2.0547	1.8453	2.2181	2.1472	2.1891	2.2957
R^2	0.9971	0.9973	0.9948	0.9987	0.9992	0.9991
χ^2	4.06×10^{-4}	3.93×10^{-4}	8.17×10^{-4}	1.85×10^{-4}	1.22×10^{-4}	1.44×10^{-4}
RSS	0.00974	0.00903	0.01634	0.005	0.00294	0.00317
Page model						

(Continues)

TABLE 2 | (Continued)

	Control			PAW-treated		
Air flow (m/s)	**0.3**	**0.6**	**0.9**	**0.3**	**0.6**	**0.9**
k	8.56×10^{-5}	6.51×10^{-5}	5.62×10^{-5}	1.87×10^{-5}	1.45×10^{-5}	1.17×10^{-5}
n	1.7975	1.8805	1.9410	2.0204	2.1015	2.1721
R^2	0.9952	0.9948	0.9913	0.9979	0.9986	0.9981
χ^2	6.10×10^{-4}	6.77×10^{-4}	0.00119	2.69×10^{-4}	1.91×10^{-4}	2.71×10^{-4}
RSS	0.0164	0.0175	0.0272	0.00807	0.00515	0.00676
Drying temperature: 70°C						
Logarithmic model						
a	0.0562	0.0712	0.0630	0.0443	0.0456	0.0388
b	1.0199	1.0443	1.0292	1.0240	1.0208	1.0002
k	0.0238	0.0248	0.0289	0.0212	0.0227	0.0257
R^2	0.9968	0.9977	0.9972	0.9979	0.9974	0.9967
χ^2	4.62×10^{-4}	3.26×10^{-4}	4.20×10^{-4}	2.83×10^{-4}	3.70×10^{-4}	4.59×10^{-4}
RSS	0.00924	0.00522	0.00630	0.00509	0.00629	0.00689
Combined two-term exponential model						
a	0.4789	0.4818	0.4795	0.4858	0.4838	0.4776
b	0.4788	0.4818	0.4794	0.4859	0.4838	0.4777
k	2.18×10^{-5}	4.18×10^{-5}	4.31×10^{-5}	7.53×10^{-6}	9.75×10^{-6}	7.84×10^{-6}
h	2.18×10^{-5}	4.18×10^{-5}	4.31×10^{-5}	7.53×10^{-6}	9.75×10^{-6}	7.84×10^{-6}
n	2.1492	2.0610	2.1076	2.2816	2.2650	2.3447
R^2	0.9963	0.9973	0.9965	0.9974	0.9969	0.9957
χ^2	6.00×10^{-4}	4.49×10^{-4}	5.99×10^{-4}	4.05×10^{-4}	4.87×10^{-4}	6.92×10^{-4}
RSS	0.0108	0.00628	0.00779	0.00648	0.00731	0.009
Page model						
k	5.59×10^{-5}	8.96×10^{-5}	1.02×10^{-4}	1.57×10^{-5}	2.20×10^{-5}	2.56×10^{-5}
n	1.9718	1.9152	1.9386	2.1469	2.1141	2.1201
R^2	0.9940	0.9955	0.9944	0.9958	0.9950	0.9921
χ^2	8.30×10^{-4}	6.16×10^{-4}	7.92×10^{-4}	5.51×10^{-4}	6.69×10^{-4}	0.00105
RSS	0.01744	0.01047	0.01267	0.01047	0.01204	0.01677

Note: Where a, b, h, n, and k, rate constants; R^2, coefficient of determination; *RSS*, residual sum of squares; χ^2, reduced chi-square.
Abbreviation: PAW, plasma-activated water.

material during the drying process. The D_{eff} relationship with temperature and air velocity plays a crucial role in optimizing drying conditions [47]. The observed increase in D_{eff} with rising temperature (50°C, 60°C, and 70°C) and air velocity (0.3, 0.6, and 0.9 m/s) across both treated and control samples is in line with established drying kinetics theory. Although elevated temperatures significantly enhance moisture removal in the early stages of drying by accelerating evaporation, a noticeable decline in moisture removal is observed during the later stages. This reduction is likely due to the formation of a hardened surface layer, which restricts internal moisture migration.

The values of D_{eff} for the control and treated samples ranged from 9.913×10^{-9} to 6.939×10^{-9} m²/s and 9.582×10^{-9} to 5.782×10^{-9} m²/s, respectively. It reflects the enhanced moisture transfer capabilities associated with higher temperatures. This increase in D_{eff} with temperature can be attributed to the enhanced activity of water molecules, which can move more rapidly at higher temperatures due to the additional thermal energy supplied [48]. The increase in thermal energy raises the vapor pressure of water, facilitating moisture diffusion from the interior of the PDSOPP particles toward the surface. This result is consistent with previous studies, which have found a positive correlation between temperature and effective diffusivity in drying processes of various organic materials, including fruits and vegetables [49].

The differences in D_{eff} between the treated and control samples indicate that the treatment may have influenced the material's microstructure, potentially increased its surface area, or altered its pore structure. This change could enhance the rate of moisture transfer, which is especially relevant when

TABLE 3 | Effective moisture diffusivity (D_{eff}), activation energy (E_a), and overall drying time of control and PAW-treated samples.

Samples	D_{eff} (m^2/s)	E_a (kJ/mol)	Overall drying time (min)
DE_1C	5.782×10^{-9}	39.27	420
DE_4C	7.600×10^{-9}		360
DE_7C	9.318×10^{-9}		330
DE_2C	6.609×10^{-9}	37.91	300
DE_5C	8.095×10^{-9}		270
DE_8C	9.417×10^{-9}		225
DE_3C	7.269×10^{-9}	36.70	210
DE_6C	8.921×10^{-9}		195
DE_9C	9.582×10^{-9}		165
DE_1	6.939×10^{-9}	36.88	465
DE_4	8.261×10^{-9}		450
DE_7	9.412×10^{-9}		390
DE_2	7.435×10^{-9}	36.12	360
DE_5	8.591×10^{-9}		315
DE_8	9.748×10^{-9}		285
DE_3	7.765×10^{-9}	35.15	255
DE_6	9.08×10^{-9}		240
DE_9	9.913×10^{-9}		225

Note: DE_1C, DE_4C, DE_7C: Control sample at 50°C (0.3, 0.6, and 0.9 m/s air velocity).
DE_2C, DE_5C, DE_8C: Control sample at 60°C (0.3, 0.6, and 0.9 m/s air velocity).
DE_3C, DE_6C, DE_9C: Control sample at 70°C (0.3, 0.6, and 0.9 m/s air velocity).
DE_1, DE_4, DE_7: Treated sample at 50°C (0.3, 0.6, and 0.9 m/s air velocity).
DE_2, DE_5, DE_8: Treated sample at 60°C (0.3, 0.6, and 0.9 m/s air velocity).
DE_3, DE_6, DE_9: Treated sample at 70°C (0.3, 0.6, and 0.9 m/s air velocity).
Abbreviation: PAW, plasma-activated water.

considering the lower D_{eff} values observed in the control samples. The increased diffusivity in treated samples is likely a result of modifications to the material's characteristics, such as the breakdown of cell walls or the creation of more porous structures, which facilitate moisture movement [50]. The experimental data for D_{eff} and the reciprocal of temperature ($1/T$) were further used to calculate the activation energy (E_a) using the slope method (Table 3). The activation energy represents the amount of energy needed to drive the moisture diffusion process, with lower E_a values indicating that the drying process becomes easier or more efficient at lower temperatures [51]. In this study, the E_a values for the control samples were found to be 39.27, 37.91, and 36.70 kJ/mol, while for the treated samples, they were slightly lower at 36.88, 36.12, and 35.12 kJ/mol. The trend of lower E_a values in the treated samples suggests that the drying process in these samples requires less energy to initiate moisture diffusion. It is likely due to the structural modifications induced by the PAW treatment. This result is consistent with findings from other studies, where lower activation energy values were reported for apricots (31.4 kJ/mol) and dried carrots (35.53 kJ/mol) in hot-air drying without any pretreatment [52, 53].

The reduction in E_a for treated samples indicates that the treatment could have facilitated the drying process by making the material more susceptible to moisture loss at lower temperatures. This is an important consideration when optimizing drying methods; a lower E_a value can lead to more energy-efficient drying processes. The observed variability in E_a values across different drying conditions is likely due to a combination of factors (such as differences in the material's initial moisture content, maturation status, and surface area) as well as the specific drying conditions employed. These factors can all influence the rate of moisture diffusion and, consequently, the activation energy required for drying [54]. In conclusion, the results presented in this study highlight the significant impact of temperature and treatment on the effective diffusivity and activation energy of PDSOPP. The increase in D_{eff} with higher temperatures, along with the lower E_a values for treated samples, suggests that the treatment improved the drying efficiency [50]. It enhanced the moisture transfer and reduced the energy required for the process. These findings provide valuable insights into the drying kinetics of PDSOPP and can highlight the development of more efficient drying techniques [54]. The future research could explore the effects of different treatment methods on the material's microstructure. This subsequent impact on drying behavior influences the other variables, such as humidity and drying time, on the activation energy and effective diffusivity.

3.4 | Total Phenols and Flavonoid Content

The results of this study, as shown in Table 4, provide the effect of drying kinetics on the retention of flavonoids and phenolic compounds in PDSOPP. The flavonoids and phenolic compounds are recognized for their potential health benefits and antioxidant properties, including their ability to neutralize free radicals and support various physiological functions [55]. The observed variations in the total phenolic and flavonoid content are due to changes in drying time, temperature, and air velocity. It emphasizes the delicate balance between optimizing drying conditions and preserving the bioactive compounds present in the material [56]. The total phenolic content in the control samples ranged from 77.51 mg GAE/100 g to 102.30 mg GAE/100 g, and in the treated samples, it ranged from 83.47 mg GAE/100 g to 110.12 mg GAE/100 g. The data reveal a noticeable trend as the drying time decreased (from 380 min at DE_1C to 225 min at DE_6C); the total phenolic content increased in both control and treated samples. This suggests that shorter drying times, especially those below a critical threshold, may help retain phenolic compounds. The increase in phenolic content during the initial stages of drying could be due to the breakdown of cell walls and the concentration of bioactive compounds as moisture content decreases [56, 57]. However, as drying time continued to reduce beyond certain points (DE_7C to DE_9C), a decline in phenolic content was observed, especially under higher temperature (70°C) and increased air velocities (0.3, 0.6, and 0.9 m/s).

The observed decrease in phenolic content at longer drying times or higher drying intensities is consistent with findings reported by Deng et al. [17], who noted a reduction in total phenolic content in lemon peels. The decline of phenolic compounds is likely attributed to thermal degradation and oxidation during the drying process. It is observed particularly

TABLE 4 | Total phenol content (TPC), total flavonoid content (TFC), and antioxidant activity (AOA) of control and PDSOPP.

Samples	TPC (mg GAE/100 g)	TFC (mg QE/100 g)	AOA (% DPPH)	FRAP (μg AA/g)
DE_1C	77.51 ± 3^{l}	294.07 ± 1.89^{m}	32.92 ± 2.67^{e}	67.88 ± 2.17^{h}
DE_2C	82.31 ± 1.84^{jkl}	308.17 ± 2.4^{l}	33.11 ± 2.33^{e}	69.07 ± 0.99^{h}
DE_3C	87.42 ± 2.59^{hij}	311.44 ± 1.84^{l}	34.05 ± 1.04^{e}	71.82 ± 2.17^{gh}
DE_4C	80.66 ± 2.51^{kl}	309.24 ± 2.54^{l}	34.09 ± 2.27^{ce}	72.32 ± 1.91^{gh}
DE_5C	85.53 ± 1.6^{ijk}	321.13 ± 3.48^{j}	34.12 ± 1.06^{e}	73.27 ± 1.82^{gh}
DE_6C	102.3 ± 1.84^{bcd}	370.18 ± 4.6^{g}	35.87 ± 1.41^{bcd}	80.72 ± 1.32^{f}
DE_7C	94.17 ± 1.81^{fg}	351.82 ± 2.54^{i}	34.2 ± 1.73^{cde}	77.1 ± 2.7^{fg}
DE_8C	96.42 ± 1.03^{defg}	363.54 ± 4.04^{h}	34.05 ± 1.69^{de}	76.17 ± 2.04^{fg}
DE_9C	92.09 ± 1.04^{gh}	337.03 ± 2.6^{i}	33.7 ± 1.7^{de}	75.09 ± 1.02^{fg}
DE_1	83.47 ± 2.06^{abc}	451.63 ± 0.54^{b}	44.93 ± 1.95^{ab}	103.72 ± 1.27^{bc}
DE_2	87.24 ± 2.15^{ab}	462.47 ± 2.57^{a}	45.1 ± 0.61^{ab}	106.18 ± 1.08^{ab}
DE_3	90.83 ± 3.65^{a}	470.36 ± 3^{a}	46.77 ± 0.99^{a}	107.22 ± 1.75^{a}
DE_4	95.63 ± 1.78^{efg}	$477.56 \pm 2.04^{d,e}$	46.92 ± 2.03^{ab}	108.45 ± 2.09^{bcde}
DE_5	98.75 ± 2.73^{def}	483.12 ± 2.25^{cd}	47.5 ± 1.54^{ab}	110.07 ± 2.72^{bcd}
DE_6	110.12 ± 1.49^{jkl}	510.47 ± 2.87^{g}	48.72 ± 1.68^{abc}	118.67 ± 2.06^{e}
DE_7	107.44 ± 1.32^{hij}	504.79 ± 1.96^{f}	47.28 ± 2.79^{abc}	114.11 ± 1.91^{de}
DE_8	105.87 ± 1.13^{ghi}	492.2 ± 1.69^{ef}	45.11 ± 0.71^{abc}	112.37 ± 2.28^{de}
DE_9	100.06 ± 1.5^{cde}	488.1 ± 1.03^{bc}	43.92 ± 1.51^{ab}	110.43 ± 1.6^{bcd}

Note: Different letters in the same column showed significant ($p < 0.05$) differences between the samples.
Abbreviations: AA, ascorbic acid; DPPH, 2,2-diphenyl-1-picrylhydrazyl; FRAP, ferric reducing antioxidant power; GAE, gallic acid equivalent; PAW, plasma-activated water; PDSOPP, PAW-treated debittered sweet orange peel powder; QE, quercetin equivalent.

at higher temperatures, which are known to be sensitive to heat. The phenolic compounds are susceptible to thermal damage, and prolonged exposure to high temperatures may result in their degradation (loss of antioxidant activity). Therefore, although short drying times help retain phenolic compounds, careful control of the process is essential to avoid excessive heat-induced degradation [54, 58]. Flavonoids, another group of bioactive compounds, are prevalent in sweet orange peel, important for their ability to neutralize ROS [59]. The total flavonoid content increased with reduced drying time for both control and treated samples. In control samples, the flavonoid content rose from 294.07 mg QE/100 g to 370.18 mg QE/100 g, while in treated samples, it increased from 451.63 mg QE/100 g to 510.47 mg QE/100 g. The observed increase in flavonoid content with decreasing drying time suggests that the faster removal of moisture can help preserve the flavonoids [60]. They are less likely to undergo thermal degradation in the early stages of drying.

A decline in flavonoid content was noted in both the control (DE_7C–DE_9C) and treated (DE_7–DE_9) samples at the highest drying times, particularly under higher temperatures (70°C) and increased air flow rates (0.3, 0.6, and 0.9 m/s). This decline is likely due to the sensitivity of flavonoids to heat, as prolonged exposure to high temperatures can lead to the breakdown of these compounds, as suggested by Özcan et al. [18]. The study by Özcan et al. [18] demonstrated that drying methods, such as oven, microwave, and infrared drying, could lead to an increase in total flavonoid content in orange and lemon peel powder. The drying conditions were optimized to prevent excessive heat damage. Similarly, our results suggest that the reduced drying time is beneficial for preserving flavonoids. The excessively high temperatures and prolonged drying durations may negate these benefits, leading to the degradation of the flavonoid compounds [60]. The findings underscore the delicate interaction between drying time, temperature, and air velocity in preserving the bioactive compounds in PDSOPP. The shorter drying times help retain higher levels of both phenolic compounds and flavonoids. The excessive drying time and higher temperatures can lead to a significant loss of these valuable bioactive molecules. This highlights the importance of optimizing drying parameters to balance moisture removal efficiency with the preservation of the chemical integrity of bioactive compounds [54, 56].

The treatment process appears to have a positive effect on the retention of both phenolic and flavonoid content, particularly at shorter drying times. It suggests that pretreatment methods can enhance the material's ability to retain bioactive compounds during drying. The treated samples consistently exhibited higher levels of phenolics and flavonoids compared with the control samples. It could be attributed to changes in the structural properties of the material that facilitate better retention of these compounds [56, 61]. In conclusion, the results demonstrate that drying time, temperature, and air velocity significantly affect the retention of phenolic and flavonoid compounds in PDSOPP. Shorter drying times and lower temperatures are essential for preserving these bioactive compounds. The longer drying times, particularly at high temperatures, lead to their degradation. These findings align with previous research and emphasize the need for careful

optimization of drying conditions to enhance the retention of health-promoting compounds [54, 56]. Further studies could investigate alternative drying techniques or pretreatment methods to improve the preservation of phenolic and flavonoid content. It provides valuable insights for both food processing and nutritional enhancement.

3.5 | Antioxidant Activities

The antioxidant activity of orange peel (both fresh and dried) is an important aspect of its potential health benefits. The antioxidants play a crucial role in scavenging free radicals and protecting cells from oxidative damage. Free radicals, which are highly reactive molecules, can cause cellular damage and contribute to various health conditions (including aging and chronic diseases) [62]. Table 4 represents the antioxidant activity of both control and treated PDSOPP using FRAP and DPPH. The antioxidant activity measured by the FRAP and DPPH assays was significantly higher in treated samples related to the control samples. Specifically, treated samples showed an increase in DPPH scavenging activity (48.72%) and FRAP value (118.67 μg AA/g) compared with control samples (35.87% for DPPH and 80.72 μg AA/g for FRAP). This suggests that the treatment process had a positive impact on the preservation or enhancement of the antioxidant properties in the dried orange peel powder. The increased antioxidant activity in the treated samples could be due to structural changes or enhanced accessibility of antioxidant-rich molecules, phenolics, and flavonoids during the process treatment. The ROS and RON might cause cell wall disruption or modifications of cell wall membranes, improving the release and solubilization of intracellular antioxidant compounds in PAW-treated samples as compared with untreated samples [13]. The data also reveal the effect of drying conditions, particularly drying time and temperature, on antioxidant activity [63]. The samples dried at lower temperatures (50°C and 60°C) and with shorter drying times exhibited enhanced antioxidant activity in both the DPPH and FRAP assays. This trend is consistent with the general observation that lower drying temperatures can help preserve antioxidant compounds by minimizing their thermal degradation. At moderate temperatures (50°C and 60°C), the moisture removal process occurs efficiently without causing significant damage to heat-sensitive compounds like polyphenols and flavonoids [64].

The increased antioxidant activity observed in Okra pods after cold plasma treatment, as reported by Zielinska et al. [65], aligns with the notion that optimized drying or treatment conditions can help retain or even enhance antioxidant properties. In the case of orange peel, the treatment seems to have facilitated better retention of antioxidant activity. It might be possibly due to changes in the physical or chemical structure of the peel during processing, which could make antioxidant compounds more bioavailable [66]. On the other hand, at higher temperatures (70°C) and elevated air flow rates (0.3, 0.6, and 0.9 m/s), both control and treated samples showed a decrease in antioxidant activity. This decrease can be attributed to the degradation of antioxidant compounds due to prolonged exposure to high temperatures. The process of thermal degradation likely causes the breakdown of sensitive antioxidants (such as polyphenols and flavonoids), leading to a reduction in their effectiveness in neutralizing free radicals [54]. Higher temperatures can also lead to the oxidation of these compounds, further diminishing their antioxidant potential. This finding is consistent with previous research that highlighted the negative impact of high temperatures on the retention of antioxidants in dried food products. Deng et al. [17] observed a decline in antioxidant activity and total phenolic content in lemon peel after hot-air drying at elevated temperatures. In the current study, the reduction in antioxidant activity at higher drying temperatures suggests that while increased drying intensity may accelerate moisture removal, it comes at the cost of losing valuable antioxidant properties [56].

In conclusion, the results from the DPPH and FRAP assays demonstrate that drying conditions significantly influence the antioxidant activity of PDSOPP. Shorter drying times at moderate temperatures (50°C and 60°C) enhance the antioxidant activity. Higher temperatures (70°C) and elevated air velocities lead to a reduction in antioxidant properties due to thermal degradation. The treated samples consistently showed higher antioxidant activity compared with the control samples, highlighting the potential of treatment methods to preserve or even enhance the health-promoting properties of orange peel during drying. These findings underscore the importance of optimizing drying parameters to retain the bioactive compounds. It is responsible for antioxidant activity, which in turn can enhance the nutritional profile of dried food products [67]. Further research could explore alternative drying techniques (such as freeze-drying or vacuum drying) that may better preserve antioxidant activity by minimizing thermal degradation.

3.6 | Physical Properties

The results in Table 5 indicate the physical properties of PDSOPP, focusing on tapped density, bulk density, cohesion, flowability, and color parameters. These characteristics are critical for understanding the handling, processing, and storage qualities of the powder as well as how drying conditions and treatment processes affect its physical attributes. Bulk density is a key parameter in powder characterization, and it is influenced by factors such as particle size, particle size distribution, and the mass of the components [48]. The DE_6 sample was chosen for powder characterization on the basis of higher retention of polyphenols among all the samples. The bulk densities for the treated sample (DE_6) and the control sample (DE_6C) were 0.48 and 0.46 g/cm^3, respectively, indicating that the treatment process did not significantly alter the bulk density. There was only a small difference observed between the treated and control samples. These values suggest that both samples have relatively low bulk density, which is typical for dried plant-based powders that have a porous structure. This characteristic is important for the packing and storage of powders as lower bulk density. It typically indicates that greater volume per unit mass may affect packaging efficiency and storage space [56]. Tapped density measures the volume reduction of the sample when subjected to tapping, which allows the particles to settle and fill previously empty spaces [68]. For the treated sample (DE_6), the tapped density was 0.60 g/cm^3, slightly higher than the control

TABLE 5 | Physicochemical and functional properties of PDSOPP and control samples.

Physical properties	DE_6	DE_6C
Bulk density (g/cm^3)	0.48 ± 0.02^a	0.47 ± 0.01^a
Tapped density (g/cm^3)	0.60 ± 0.02^a	0.56 ± 0.01^b
Hausner ratio (HR)	1.24 ± 0.03^a	1.19 ± 0.02^b
Carr index (CRI) (%)	19.67 ± 0.05^a	16.07 ± 0.05^b
L^*	75.61 ± 0.04^a	72.30 ± 0.07^b
a^*	-0.78 ± 0.03^a	-2.13 ± 0.04^b
b^*	38.42 ± 0.04^a	36.60 ± 0.06^b
Chroma value (ΔC)	37.50 ± 1.02^a	35.56 ± 1.09^a
Water absorption capacity (g/g)	4.15 ± 0.03^a	4.16 ± 0.02^a
Swelling capacity (g/g)	6.82 ± 0.02^a	6.15 ± 0.03^b
Solubility index (g/g)	0.43 ± 0.02^a	0.40 ± 0.02^a
Oil absorption capacity (g/g)	1.33 ± 0.02^a	2.08 ± 0.02^b

Note: Alphabets followed by the same lowercase letter in the rows do not differ statistically by the T test at 5% probability.
Abbreviations: PAW, plasma-activated water; PDSOPP, PAW-treated debittered sweet orange peel powder.

sample's tapped density of 0.56 g/cm^3. This increase in tapped density for the treated sample may be attributed to changes in the particle structure induced by the treatment, which could result in a denser packing arrangement during tapping. These findings are consistent with the study by Albuquerque et al. [69], who observed similar trends in mango peel powder.

The HR is a measure of the powder's cohesiveness, and it plays a critical role in determining the flowability of powders [68]. An HR value between 1.2 and 1.4 indicates intermediate cohesion, which was observed in the treated sample with an HR value of 1.24. In contrast, the control sample exhibited lower cohesion with an HR value of 1.19, falling just below the intermediate cohesion range. According to the classification, HR values below 1.2 indicate low cohesion, while values between 1.2 and 1.4 indicate intermediate cohesion, and values above 1.4 indicate high cohesion. The observed HR values suggest that the treated sample has slightly greater cohesiveness, which may affect its flowability, potentially making it more resistant to movement during handling. This could be due to the effects of treatment, which might alter the surface characteristics or particle interactions, leading to increased particle bonding [48, 70]. The CRI is another important parameter for assessing powder flowability, with lower CRI values indicating better flowability [71]. The CRI values for the treated and control samples were 19.67% and 16.09%, respectively. On the basis of the classification, CRI values ranging from 15% to 20% signify good flow properties, whereas values between 20% and 35% are indicative of poor flowability. The treated and control samples exhibited relatively good flowability, with CRI values well within the acceptable range for powders that can be efficiently processed. The slightly higher CRI value for the treated sample suggests that it retains good flowability. The increased cohesion (as reflected in the higher HR value) might slightly reduce its ease of flow related to the control sample [72]. The findings align well with those of Albuquerque et al. [69], who reported similar CRI values for mango peel powder, indicating that the observed flowability trends are consistent with those seen in other plant-based powders.

The color parameters of the powder are also an important indicator of quality and can provide insights into the impact of drying and treatment processes [73]. The L^* (lightness), a^* (red–green), and chroma (ΔC) values were found to be enhanced in the treated samples compared with the control. It indicates that the treatment had a positive effect on the overall brightness and color intensity of the powder. The increase in L^* value suggests that the treated powder is lighter, which could be associated with the removal of certain dark pigments or the breakdown of compounds during the treatment process. Similarly, the increase in chroma (ΔC) indicates a more vibrant color in the treated samples, which might be a result of changes in the pigment composition or structure due to the treatment process. However, the b^* value (yellow–blue) was decreased in the treated samples, indicating a shift in color toward the blue end of the spectrum [74]. This could be attributed to the oxidation of pigments, which is a common occurrence in plant materials exposed to certain treatments, such as PAW and debittering treatments. These treatments may cause the decline of carotenoids and promote a more neutral or bluish tone in the powder. This color shift is consistent with findings in other studies, where treatment processes involve high energy or oxidative conditions. It resulted in alterations in the color of plant powders due to the degradation of pigments [75, 76]. PAW treatment generates reactive oxygen and nitrogen species, which can modify the surface chemistry and microstructure of the orange peel matrix. These changes can affect cellular integrity, porosity, and the availability of binding sites, all of which influence the behavior of the material during drying and subsequent powder formation. Increased porosity and surface roughness may enhance water diffusivity and promote more uniform drying. It leads to powders with improved flowability, dispersibility, or reduced particle agglomeration [13, 77].

In summary, the physical properties of the PDSOPP, including bulk density, tapped density, HR, CRI, and color parameters, were significantly influenced by drying conditions and the treatment process. The treated sample (DE_6) exhibited slight increases in bulk density and tapped density compared with the control sample (DE_6C), as well as higher cohesion (HR) and slightly reduced flowability (CRI). The color of the treated samples also exhibited enhanced lightness and chroma, along with a decrease in the yellow color component. It might be likely due to oxidation of pigments during the treatment process [74, 76]. These findings indicate that the drying conditions at 60°C with a drying time of 225 min (DE_6C) and the corresponding treated sample (DE_6) provide an optimal balance between retaining bioactive compounds and ensuring desirable physical properties in the final powder [54]. Further research could explore the impact of alternative treatment techniques on the bioactive compound retention and physical properties to further optimize the processing of orange peel powder for food and pharmaceutical applications.

3.7 | Functional Properties

The functional properties of PDSOPP play a significant role in determining its potential applications in food, pharmaceutical,

and other industries. Functional properties, such as oil WAC, OAC, SI, and SC, are critical for understanding how the powder will behave in different formulations and processes [78]. Table 5 provides valuable insights into how these properties are influenced by the drying and treatment conditions applied to the orange peel powder samples. The WAC and OAC are indicators of the powder's ability to hold water and oil, respectively. These are important for food formulations, particularly in the development of emulsions or as fat replacers in various products [79]. The results indicate that the control samples exhibited higher OAC and WAC values compared with the treated samples. Specifically, the treated samples had a lower OAC of 1.30 g/g, while the control samples had a higher OAC (2.07 g/g). Similarly, the WAC for the treated samples was lower than that of the control samples. The higher OAC and WAC in the control samples could be attributed to the presence of protein structures and nonpolar amino acids in the untreated orange peel powder. These proteins and amino acids are known to interact with water and oil molecules, promoting greater absorption [80]. These properties in the control samples might also be due to the inherent structure and composition of the untreated orange peel. It retains more hydrophilic and lipophilic sites, thus facilitating better absorption of both water and oil. The treated samples exhibited lower OAC and WAC values, which may reflect changes in the structural properties of the powder caused by the treatment. The treatment process (such as the use of PAW or other physical treatments) could have modified the cell wall structure, reducing the powder's capacity to absorb water and oil. This could be due to the breakdown of certain molecular structures, such as proteins or carbohydrates, that contribute to the retention of these fluids [81].

SC is an important functional properties that reflect the powder's ability to absorb water and expand in size. This property is especially relevant for applications involving the development of gels or hydrogels [82]. In the present study, the SC of the control samples was 6.82 g/g, while the SC for the treated samples was 6.15 g/g. Similarly, the SI for the control samples was 0.43 g/g, whereas it was slightly lower for the treated samples at 0.40 g/g. Although the treated samples had marginally lower SC and SI values compared with the control, the values were relatively close. It indicates that the treatment did not drastically reduce the swelling ability of the samples. One possible explanation for the slight difference is that the reduction in moisture content during drying, particularly in the treated samples, might have led to a higher concentration of soluble components (such as dietary fiber and carbohydrates) in the PDSOPP. The remaining soluble compounds, which are often responsible for water retention and swelling, become more concentrated as the moisture is removed. This increased concentration may enhance the swelling power and stability of the treated samples, even though the overall SC and SI values were slightly lower than those of the control samples [83].

Bie et al. [84] stated that both oxidation and molecular degradation of polysaccharides induced by active plasma species or similar treatments could contribute to greater stability and swelling properties in treated materials. This aligns with the current findings, where treatment-induced changes in the molecular structure might have contributed to improved stability and maintained a good level of SC despite the reduction in moisture content. In conclusion, the functional properties of PDSOPP are significantly impacted by both the drying and treatment conditions. The control samples exhibited higher oil and water absorption capacities, while the treated samples demonstrated comparable swelling properties. It suggested that the treatment process enhanced the concentration of soluble components (such as dietary fiber), which contributed to the swelling power and stability [85]. The observed reduction in OAC and WAC in treated samples might be due to changes in the structural integrity of the powder, possibly caused by the treatment process [86]. These findings are consistent with previous research, such as that by Bie et al. [84], which indicated that treatment processes can alter functional properties like absorption capacity and swelling. Further research could explore additional treatment methods or drying techniques that might optimize these functional properties for specific applications in food processing and other industries.

3.8 | SEM and XRD Analysis of PDSOPP

The morphological and crystallographic characteristics of PDSOPP were examined through SEM and XRD analysis, providing valuable insights into the structural changes induced by the treatment process. The SEM images of the PDSOPP samples (Figure 2A,B) revealed notable differences between the control and treated samples. In the control samples, the powder particles appeared compact and dense, suggesting a more tightly packed structure. In contrast, the treated samples exhibited a more porous and less compact structure with visible spaces between the particles. This change in particle morphology could have significant implications for the bioavailability and release of bioactive compounds (such as flavonoids and polyphenols) [87]. The increased porosity in the treated samples could facilitate the easier release and extraction of these compounds. The more open structure may allow for improved accessibility to the cellular components responsible for the retention of polyphenols and flavonoids. This morphological transformation is likely a result of the interaction of reactive plasma species, particularly ROS and RNS, during the treatment process [88]. These species are known to induce changes in the physical structure of plant materials by breaking down cellular walls and altering the arrangement of molecules within the matrix. The previous studies have indicated that treatments involving plasma species can lead to increased porosity and altered particle size distributions in plant-based powders. It is consistent with the findings observed in this study. The enhanced porosity in the treated samples could therefore improve their functionality in various applications, particularly those that rely on the release of bioactive compounds [56].

The XRD patterns of the PDSOPP samples (Figure 3A) revealed differences in the crystalline structure between the control and treated samples. The XRD peaks observed at 2θ values of 18.40°, 20.90°, 25.16°, and 24.98° are indicative of the characteristic crystalline regions in the orange peel powder. The CI was calculated to be 18.09% for the control samples and 21.45% for the treated samples. This increase in crystallinity for the treated samples suggests that the treatment process induced changes in the crystalline structure of the PDSOPP. The higher crystallinity in the treated samples may result from the alteration of amorphous regions into more ordered crystalline structures during

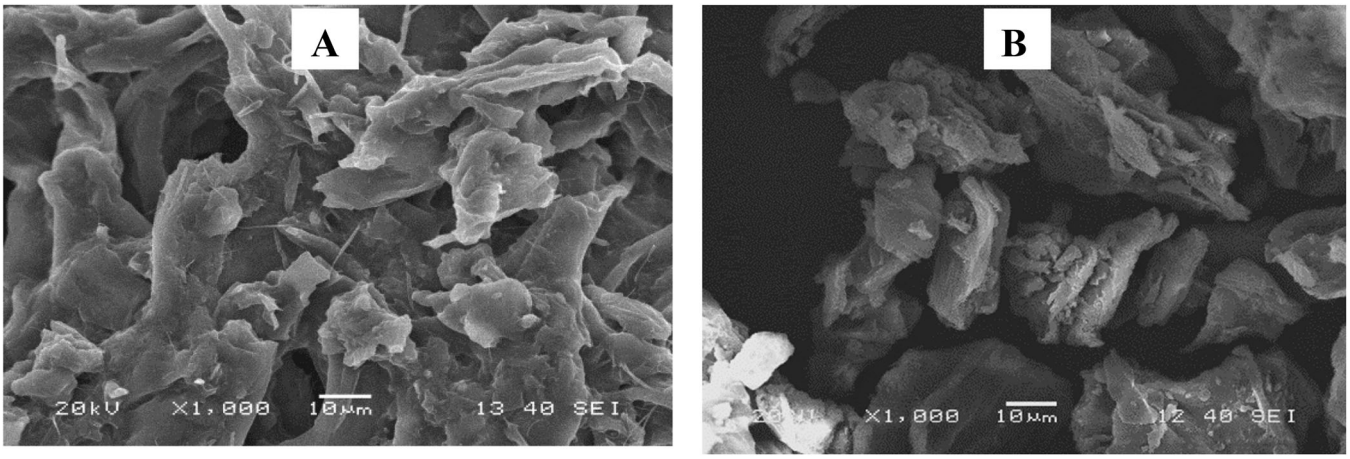

FIGURE 2 | Scanning electron microscopy images of 60°C (with an air velocity of 0.9 m/s) dried samples: (A) PAW-untreated and (B) with PAW-treated. PAW, plasma-activated water.

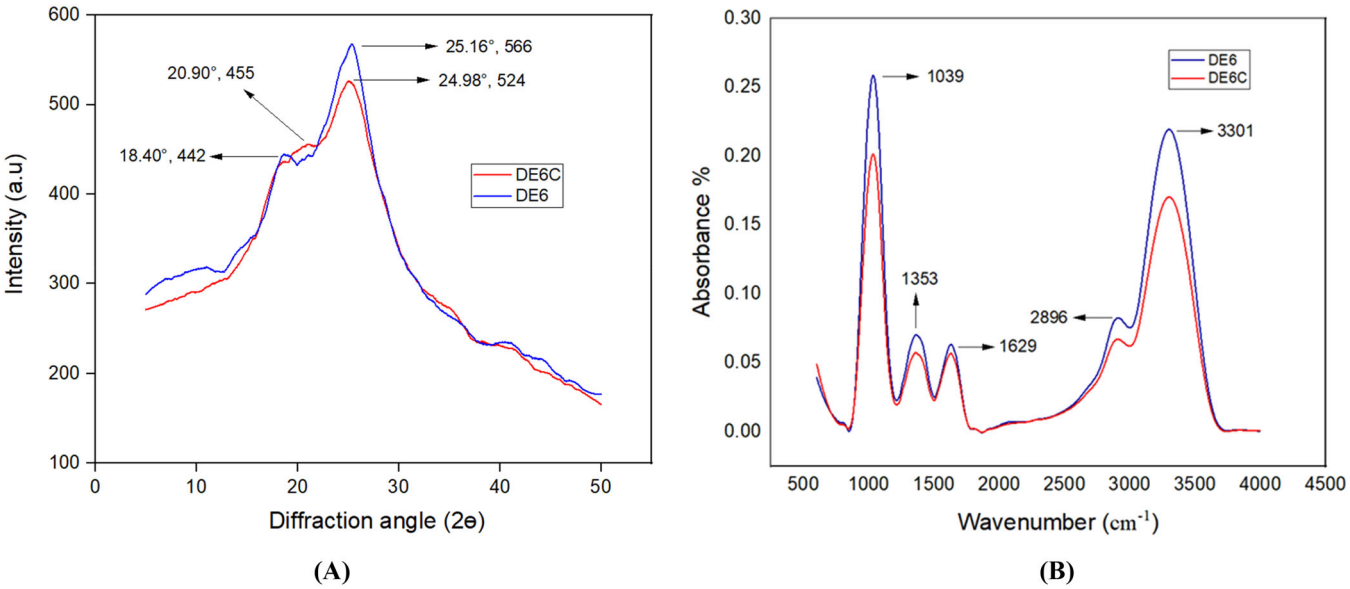

(A) **(B)**

FIGURE 3 | (A) XRD pattern and (B) FTIR spectrum of sweet orange peel powder samples. FTIR, Fourier-Transform Infrared; XRD, X-ray diffraction.

the treatment process. This phenomenon is often observed in materials exposed to physical treatments (such as plasma-assisted processes), where the application of energy can lead to the reorganization of molecular structures [89]. Similar findings have been reported by other researchers, where treatments involving plasma or similar energy-based techniques were shown to enhance the crystallinity of plant-based materials. It is likely due to the rearrangement of cellulose and other polysaccharides into more ordered structures. The increased crystallinity observed in the treated PDSOPP could impact its functional properties (such as solubility and digestibility), which are influenced by the degree of crystallinity in the powder [90].

In summary, the morphological and crystallographic analysis of PDSOPP has provided valuable insights into the effects of the treatment process on the structure of the powder. The treated samples exhibited increased porosity and crystallinity compared with the control samples. It may enhance the release and bioavailability of bioactive compounds, such as polyphenols and flavonoids [56]. These structural changes are likely a result of the interaction of reactive plasma species during treatment. It can induce both physical and chemical modifications in plant materials. The observed increase in crystallinity and porosity suggests that the treated PDSOPP may have improved functionality for applications in food, pharmaceutical, and other industries where bioactive compound release and structural properties are critical [88]. Further studies could explore the specific mechanisms behind these structural changes and their impact on the functional and nutritional properties of the powder.

3.9 | FTIR Spectrum of PDSOPP

The FTIR analysis of PDSOPP (DE_6 and DE_6C) provided detailed information about the chemical functional groups present in the treated and control samples. The FTIR spectra shown in

Figure 3B revealed several distinct peaks that are characteristic of various bioactive compounds and macromolecules. It offers insight into the structural changes and chemical composition of the orange peel powder before and after treatment. The FTIR spectra of control (DE_6C) and both treated (DE_6) samples exhibited a broad peak at 3301/cm, which corresponds to the O─H stretching vibration of phenolic compounds. This broad band is indicative of the presence of hydroxyl groups commonly found in polyphenols and flavonoids, which are key bioactive components in orange peel. The broadness of this peak suggests strong hydrogen bonding, likely due to the hydroxyl groups interacting with water molecules or other functional groups present in the sample [59]. The presence of peaks at 2896/cm is associated with C─H stretching, which is characteristic of aliphatic hydrocarbons. This absorption is likely related to the fatty acids, lipids, or other aliphatic components present in the orange peel, contributing to the overall molecular structure of the powder. Similarly, the peak at 1629/cm, which is indicative of C═O stretching in conjugated carbonyl groups, can be associated with the presence of proteins, lipids, or other carbonyl-containing compounds within the orange peel powder.

The prominent peak at 1353/cm corresponds to C─O bonding and O─H stretching of carbohydrates and polysaccharides, which are abundant in orange peel. These peaks suggest that the treated and control samples contain significant amounts of cellulose, hemicellulose, and pectin, which are important polysaccharides that contribute to the functional properties and structural integrity of plant materials [91]. The peak at 1039/cm further supports the presence of C─O stretching vibrations, likely related to the polysaccharide components in the peel, such as cellulose and pectin. The observed FTIR peaks in the PDSOPP samples are consistent with those reported for various citrus fruits. Specifically, similar absorption bands ranging from 1700 to 1500/cm (C═O stretching), 1500 to 1300/cm (C─H stretching), and 1150 to 950/cm (C─O bonding) have been observed in citrus peel samples [92]. These results confirm the presence of typical functional groups, such as carbonyl, hydroxyl, and polysaccharide structures, in both the treated and control orange peel powders. The consistency in these absorption patterns further supports the notion that the chemical composition of PDSOPP is largely retained after treatment. The slight modifications to the molecular structure could occur as reflected in the changes in morphology and crystallinity [93]. The FTIR analysis of PDSOPP samples has provided valuable insights into the chemical composition of the powder. It highlights the presence of phenolic compounds, polysaccharides, and other bioactive compounds. The broad O─H stretching peak at 3301/cm, along with peaks corresponding to C─H stretching, C═O stretching, and C─O stretching, confirms the retention of key bioactive components in both treated and control samples. It confirms the retention of key bioactive components, such as polyphenols, flavonoids, and carbohydrates, in both treated and control samples. The similarity of these spectra to those observed in other citrus fruit samples reinforces the characterization of PDSOPP as a rich source of bioactive compounds [54]. Furthermore, the subtle structural changes observed in the FTIR spectra may contribute to the enhanced bioactivity of the treated samples. It is reflected in their increased antioxidant and phenolic content. These findings underscore the potential of PDSOPP for various applications in the food, pharmaceutical, and nutraceutical industries.

4 | Conclusion

This study comprehensively evaluated the drying characteristics, functional properties, and bioactive compound retention of PDSOPP under varying drying conditions. The results showed that the drying process significantly influences the retention of bioactive compounds, such as flavonoids, phenolic compounds, and antioxidant activities in orange peel powder. The optimized drying condition, specifically DE_6 (drying time of 285 min, airflow of 0.9 m/s at 60°C), demonstrated the highest retention of these beneficial compounds. Thus, offering a promising approach to enhance the functional properties of PDSOPP. The morphological analysis using SEM revealed that the treated samples exhibited greater porosity compared with the control. It is likely beneficial for the release and bioavailability of polyphenols and flavonoids. Furthermore, the XRD analysis exhibited an increase in crystallinity in the treated samples. It indicated structural changes induced by the drying process. The FTIR analysis further confirmed the presence of key functional groups, such as carbonyl and hydroxyl groups, which are associated with the bioactive compounds in orange peel. In terms of physical properties, the treated PDSOPP samples showed a slight decrease in bulk and swelling capacities but maintained good flowability. It suggested that the treatment process improved the powder's suitability for various applications. Additionally, the antioxidant activity determined by the FRAP and DPPH assays was enhanced in the treated samples. It confirmed the beneficial effects of optimized drying conditions on the preservation of antioxidants. Overall, the findings from this study suggest that PDSOPP, particularly when dried under optimized conditions, retains its nutritional and functional properties. It can be considered a valuable resource for the food, pharmaceutical, and nutraceutical industries. Future studies should investigate the molecular and structural mechanisms driving the changes induced by the treatment process and further assess the potential of PDSOPP in different product formulations.

Author Contributions

Venkatraman Bansode: conceptualization, investigation, writing – original draft. **S. Ganga Kishore:** writing – original draft, data curation, methodology. **Rahul Rajkumar:** data analysis, modeling, and formatting. **Madhuresh Dwivedi:** supervision, review and editing. **Rama Chandra Pradhan:** supervision, resources. **Robbarts Nongmaithem:** formal analysis, data analysis. **Jeevarathinam Ganesan:** formal analysis, review and editing. **Deepa Jaganathan:** formal analysis.

Acknowledgments

The authors are thankful to Dr. D. K. Ghosh, Director, ICAR-Central Citrus Research Institute, Nagpur, Maharashtra, India, for granting study leave and necessary facilities at his institute.

Conflicts of Interest

The authors declare no conflicts of interest.

Data Availability Statement

The data that support the findings of this study are available from the corresponding author upon reasonable request.

References

1. P. Bhattacharjee, M. J. Patel, O. Warang, N. J. Jadav, and S. Debbarma, "Impact of Integrated Nutrient Management on Yield, Soil, and Plant Nutrient Status in Sweet Orange (*Citrus sinensis* L.) cv. Phule Mosambi," *Communications in Soil Science and Plant Analysis* 55, no. 16 (2024): 2379–2392, https://doi.org/10.1080/00103624.2024.2359578.

2. S. Seminara, S. Bennici, M. Di Guardo, et al., "Sweet Orange: Evolution, Characterization, Varieties, and Breeding Perspectives," *Agriculture (London)* 13, no. 2 (2023): 264, https://doi.org/10.3390/agriculture13020264.

3. T. O. Ogunbode, V. I. Esan, M. H. Ayegboyin, O. M. Ogunlaran, E. T. Sangoyomi, and J. A. Akande, "Analysis of Farmers' Perceptions on Sustainable Sweet Orange Farming in Nigeria Amid Climate Change," *Scientific Reports* 15, no. 1 (2025): 5205, https://doi.org/10.1038/s41598-025-90056-6.

4. H. Kato-Noguchi and M. Kato, "Pesticidal Activity of Citrus Fruits for the Development of Sustainable Fruit-Processing Waste Management and Agricultural Production," *Plants* 14, no. 5 (2025): 754, https://doi.org/10.3390/plants14050754.

5. P. Sharma, R. Vishvakarma, K. Gautam, et al., "Valorization of Citrus Peel Waste for the Sustainable Production of Value-Added Products," *Bioresource Technology* 351 (2022): 127064, https://doi.org/10.1016/j.biortech.2022.127064.

6. O. Figueira, V. Pereira, and P. C. Castilho, "A Two-Step Approach to Orange Peel Waste Valorization: Consecutive Extraction of Pectin and Hesperidin," *Foods* 12, no. 20 (2023): 3834, https://doi.org/10.3390/foods12203834.

7. S. K. Khanal, S. Varjani, C. Sze Ki Lin, and M. K. Awasthi, "Waste-to-Resources: Opportunities and Challenges," *Bioresource Technology* 317 (2020): 123987, https://doi.org/10.1016/j.biortech.2020.123987.

8. S. Varjani, P. Rakholiya, H. Yong Ng, et al., "Bio-Based Rhamnolipids Production and Recovery From Waste Streams: Status and Perspectives," *Bioresource Technology* 319 (2021): 124213, https://doi.org/10.1016/j.biortech.2020.124213.

9. P. Dubey, G. Tripathi, S. S. Mir, and O. Yousuf, "Current Scenario and Global Perspectives of Citrus Fruit Waste as a Valuable Resource for the Development of Food Packaging Film," *Trends in Food Science & Technology* 141 (2023): 104190, https://doi.org/10.1016/j.tifs.2023.104190.

10. N. Medina-Herrera, G. C. G. Martínez-Ávila, C. L. Robledo-Jiménez, R. Rojas, and B. S. Orozco-Zamora, "From Citrus Waste to Valuable Resources: A Biorefinery Approach," *Biomass* 4, no. 3 (2024): 784–808, https://doi.org/10.3390/biomass4030044.

11. N. Mahato, K. Sharma, M. Sinha, and M. H. Cho, "Citrus Waste Derived Nutra-/Pharmaceuticals for Health Benefits: Current Trends and Future Perspectives," *Journal of Functional Foods* 40 (2018): 307–316, https://doi.org/10.1016/j.jff.2017.11.015.

12. B. Singh, J. P. Singh, A. Kaur, and M. P. Yadav, "Insights into the Chemical Composition and Bioactivities of Citrus Peel Essential Oils," *Food Research International* 143 (2021): 110231, https://doi.org/10.1016/j.foodres.2021.110231.

13. V. Bansode, S. Jaddu, T. Chandra Panda, et al., "Hurdle Approach of Plasma-Activated Water Pretreatment With Debittering Treatment on Naringin and Limonin Content of Sweet Orange Peel Powder," *Food Bioscience* 60 (2024): 104431, https://doi.org/10.1016/j.fbio.2024.104431.

14. R. Thirumdas, A. Kothakota, U. Annapure, et al., "Plasma Activated Water (PAW): Chemistry, Physico-Chemical Properties, Applications in Food and Agriculture," *Trends in Food Science & Technology* 77 (2018): 21–31, https://doi.org/10.1016/j.tifs.2018.05.007.

15. R. Farahmandfar, B. Tirgarian, B. Dehghan, and A. Nemati, "Comparison of Different Drying Methods on Bitter Orange (*Citrus aurantium* L.) Peel Waste: Changes in Physical (Density and Color) and Essential Oil (Yield, Composition, Antioxidant and Antibacterial) Properties of Powders," *Journal of Food Measurement and Characterization* 14 (2020): 862–875, https://doi.org/10.1007/s11694-019-00334-x.

16. L. Y. W. Chua, C. H. Chong, B. L. Chua, and A. Figiel, "Influence of Drying Methods on the Antibacterial, Antioxidant and Essential Oil Volatile Composition of Herbs: A Review," *Food and Bioprocess Technology* 12 (2019): 450–476, https://doi.org/10.1007/s11947-018-2227-x.

17. L. Z. Deng, A. S. Mujumdar, W. X. Yang, et al., "Hot Air Impingement Drying Kinetics and Quality Attributes of Orange Peel," *Journal of Food Processing and Preservation* 44, no. 1 (2020): e14294, https://doi.org/10.1111/jfpp.14294.

18. M. M. Özcan, K. Ghafoor, F. Al Juhaimi, et al., "Influence of Drying Techniques on Bioactive Properties, Phenolic Compounds and Fatty Acid Compositions of Dried Lemon and Orange Peel Powders," *Journal of Food Science and Technology* 58 (2021): 147–158, https://doi.org/10.1007/s13197-020-04524-0.

19. G. Guclu, S. Polat, H. Kelebek, E. Capanoglu, and S. Selli, "Elucidation of the Impact of Four Different Drying Methods on the Phenolics, Volatiles, and Color Properties of the Peels of Four Types of Citrus Fruits," *Journal of the Science of Food and Agriculture* 102, no. 13 (2022): 6036–6046, https://doi.org/10.1002/jsfa.11956.

20. V. Phuon, I. N. Ramos, T. R. S. Brandão, and C. L. M. Silva, "Assessment of the Impact of Drying Processes on Orange Peel Quality Characteristics," *Journal of Food Process Engineering* 45, no. 7 (2022): e13794, https://doi.org/10.1111/jfpe.13794.

21. N. F. Abd Rahman, R. Shamsudin, A. Ismail, N. N. A. K. Shah, and J. Varith, "Effects of Drying Methods on Total Phenolic Contents and Antioxidant Capacity of the Pomelo (*Citrus grandis* (L.) Osbeck) Peels," *Innovative Food Science & Emerging Technologies* 50 (2018): 217–225, https://doi.org/10.1016/j.ifset.2018.01.009.

22. V. Bansode, T. Chandra Panda, S. Jaddu, et al., "Enhancing Nutritional Potential: Plasma-Activated Water Treatment on Sweet Orange Peel Powder—Polyphenols, Flavonoids, Antioxidants, and Anti-Nutrients Optimization," *IEEE Transactions on Plasma Science* 53 (2025): 51–62, https://doi.org/10.1109/TPS.2024.3523670.

23. H.-Y. Ju, H. M. El-Mashad, X.-M. Fang, et al., "Drying Characteristics and Modeling of Yam Slices Under Different Relative Humidity Conditions," *Drying Technology* 34, no. 3 (2016): 296–306, https://doi.org/10.1080/07373937.2015.1052082.

24. J.-W. Bai, D.-W. Sun, H.-W. Xiao, A. Mujumdar, and Z.-J. Gao, "Novel High-Humidity Hot Air Impingement Blanching (HHAIB) Pretreatment Enhances Drying Kinetics and Color Attributes of Seedless Grapes," *Innovative Food Science & Emerging Technologies* 20 (2013): 230–237, https://doi.org/10.1016/j.ifset.2013.08.011.

25. L.-Z. Deng, X.-H. Yang, A. S. Mujumdar, et al., "Red Pepper (*Capsicum annuum* L.) Drying: Effects of Different Drying Methods on Drying Kinetics, Physicochemical Properties, Antioxidant Capacity, and Microstructure," *Drying Technology* 36, no. 8 (2018): 893–907, https://doi.org/10.1080/07373937.2017.1361439.

26. L. Xie, Z.-A. Zheng, A. S. Mujumdar, et al., "Pulsed Vacuum Drying (PVD) of Wolfberry: Drying Kinetics and Quality Attributes," *Drying Technology* 36, no. 12 (2018): 1501–1514, https://doi.org/10.1080/07373937.2017.1414055.

27. S. Padhi and M. Dwivedi, "Physico-Chemical, Structural, Functional and Powder Flow Properties of Unripe Green Banana Flour After the Application of Refractance Window Drying," *Future Foods* 5 (2022): 100101, https://doi.org/10.1016/j.fufo.2021.100101.

28. S. N. Bhusari, K. Muzaffar, and P. Kumar, "Effect of Carrier Agents on Physical and Microstructural Properties of Spray Dried Tamarind Pulp Powder," *Powder Technology* 266 (2014): 354–364, https://doi.org/10.1016/j.powtec.2014.06.038.

29. M. Smita, M. Bashir, and S. Haripriya, "Physicochemical and Functional Properties of Peeled and Unpeeled Coconut Haustorium Flours," *Journal of Food Measurement and Characterization* 13, no. 1 (2019): 61–69, https://doi.org/10.1007/s11694-018-9919-9.

30. S. Jaddu, R. C. Pradhan, and M. Dwivedi, "Effect of Multipin Atmospheric Cold Plasma Discharge on Functional Properties of Little Millet (*Panicum miliare*) Flour," *Innovative Food Science & Emerging Technologies* 77 (2022): 102957, https://doi.org/10.1016/j.ifset.2022.102957.

31. S. G. Kishore, M. Dwivedi, C. G. Dalbhagat, et al., "Development of Extruded Millet Analogue Rice: A Comparison of Rheological, Structural, Physiochemical, and Cooking Properties With Conventional Rice," *ACS Food Science & Technology* 4, no. 10 (2024): 2504–2516, https://doi.org/10.1021/acsfoodscitech.4c00629.

32. S. Nigar, K. Subrahmanyam, D. B. Choudhury, K. Gul, and R. Sehrawat, "Alginate–Millet Starch Composite Matrices as Novel Carriers for Controlled Delivery of Grape Seed Polyphenols: Preparation, Characterization, and In Vitro Release Behaviour," *Food Structure* 42 (2024): 100385, https://doi.org/10.1016/j.foostr.2024.100385.

33. G. Jeevarathinam, R. Pandiselvam, T. Pandiarajan, et al., "Infrared Assisted Hot Air Dryer for Turmeric Slices: Effect on Drying Rate and Quality Parameters," *LWT* 144 (2021): 111258.

34. C. Talens, M. Castro-Giraldez, and P. J. Fito, "A Thermodynamic Model for Hot Air Microwave Drying of Orange Peel," *Journal of Food Engineering* 175 (2016): 33–42, https://doi.org/10.1016/j.jfoodeng.2015.12.001.

35. H. S. El-Mesery, "Improving the Thermal Efficiency and Energy Consumption of Convective Dryer Using Various Energy Sources for Tomato Drying," *Alexandria Engineering Journal* 61, no. 12 (2022): 10245–10261, https://doi.org/10.1016/j.aej.2022.03.076.

36. V. P. Chandramohan, "Convective Drying of Food Materials: An Overview With Fundamental Aspect, Recent Developments, and Summary," *Heat Transfer* 49, no. 3 (2020): 1281–1313, https://doi.org/10.1002/htj.21662.

37. S.-H. M. Ashtiani, M. H. Aghkhani, J. Feizy, and A. Martynenko, "Effect of Cold Plasma Pretreatment Coupled With Osmotic Dehydration on Drying Kinetics and Quality of Mushroom (*Agaricus bisporus*)," *Food and Bioprocess Technology* 16, no. 12 (2023): 2854–2876, https://doi.org/10.1007/s11947-023-03096-z.

38. D. A. Khudyakov, I. A. Shorstkii, E. E. Ulyanenko, and E. V. Gnuchykh, "Influences of Cold Atmospheric Plasma Pretreatment on Drying Kinetics, Structural, Fractional and Chemical Characteristics of Tobacco Leaves," *Drying Technology* 40, no. 15 (2022): 3285–3291, https://doi.org/10.1080/07373937.2021.2021230.

39. S. Rout, P. K. Panda, P. Dash, P. P. Srivastav, and C.-T. Hsieh, "Cold Plasma-Induced Modulation of Protein and Lipid Macromolecules: A Review," *International Journal of Molecular Sciences* 26, no. 4 (2025): 1564, https://doi.org/10.3390/ijms26041564.

40. S. Álvarez, C. Álvarez, R. Hamill, A. M. Mullen, and E. O'Neill, "Drying Dynamics of Meat Highlighting Areas of Relevance to Dry-Aging of Beef," *Comprehensive Reviews in Food Science and Food Safety* 20, no. 6 (2021): 5370–5392, https://doi.org/10.1111/1541-4337.12845.

41. G. Jeevarathinam, R. Pandiselvam, T. Pandiarajan, et al., "Design, Development, and Drying Kinetics of Infrared-Assisted Hot Air Dryer for Turmeric Slices," *Journal of Food Process Engineering* 45, no. 6 (2022): e13876, https://doi.org/10.1111/jfpe.13876.

42. J. P. Tejeda-Miramontes, B. C. Espinoza-Paredes, A. Zatarain-Palffy, T. García-Cayuela, V. Tejada-Ortigoza, and L. E. Garcia-Amezquita, "Process Modeling and Convective Drying Optimization of Raspberry Pomace as a Fiber-Rich Functional Ingredient: Effect on Techno-Functional and Bioactive Properties," *Foods* 13, no. 22 (2024): 3597, https://doi.org/10.3390/foods13223597.

43. R. Biswas, M. A. Hossain, and W. Zzaman, "Thin Layer Modeling of Drying Kinetics, Rehydration Kinetics and Color Changes of Osmotic Pre-Treated Pineapple (*Ananas comosus*) Slices During Drying: Development of a Mechanistic Model for Mass Transfer," *Innovative Food Science & Emerging Technologies* 80 (2022): 103094, https://doi.org/10.1016/j.ifset.2022.103094.

44. M. I. H. Khan, C. P. Batuwatta-Gamage, M. A. Karim, and Y. Gu, "Fundamental Understanding of Heat and Mass Transfer Processes for Physics-Informed Machine Learning-Based Drying Modelling," *Energies* 15, no. 24 (2022): 9347.

45. E. C. Tredenick and G. D. Farquhar, "Dynamics of Moisture Diffusion and Adsorption in Plant Cuticles Including the Role of Cellulose," *Nature Communications* 12, no. 1 (2021): 5042, https://doi.org/10.1038/s41467-021-25225-y.

46. G. Jeevarathinam, R. Pandiselvam, T. Pandiarajan, et al., "Infrared-Assisted Hot Air Drying of Turmeric Slices: Effects on Drying Kinetics, Quality, Efficiency, Energy Considerations, and Mathematical Modeling," *Heat Transfer* 54, no. 3 (2025): 1965–2000, https://doi.org/10.1002/htj.23261.

47. L. Meili, H. Perazzini, M. C. Ferreira, and J. T. Freire, "Analyzing the Universality of the Dimensionless Vibrating Number Based on the Effective Moisture Diffusivity and Its Impact on Specific Energy Consumption," *Heat and Mass Transfer* 56 (2020): 1659–1672, https://doi.org/10.1007/s00231-019-02787-8.

48. R. Suhag, A. Kellil, and M. Razem, "Factors Influencing Food Powder Flowability," *Powders* 3, no. 1 (2024): 65–76, https://doi.org/10.3390/powders3010006.

49. I. D. Boateng, "Recent Processing of Fruits and Vegetables Using Emerging Thermal and Non-Thermal Technologies. A Critical Review of Their Potentialities and Limitations on Bioactives, Structure, and Drying Performance," *Critical Reviews in Food Science and Nutrition* 64, no. 13 (2024): 4240–4274, https://doi.org/10.1080/10408398.2022.2140121.

50. J. O. Ighalo and A. G. Adeniyi, "A Mini-Review of the Morphological Properties of Biosorbents Derived From Plant Leaves," *SN Applied Sciences* 2, no. 3 (2020): 509, https://doi.org/10.1007/s42452-020-2335-x.

51. S. Ambawat, A. Sharma, and R. K. Saini, "Mathematical Modeling of Thin Layer Drying Kinetics and Moisture Diffusivity Study of Pretreated *Moringa oleifera* Leaves Using Fluidized Bed Dryer," *Processes* 10, no. 11 (2022): 2464, https://doi.org/10.3390/pr10112464.

52. J.-W. Dai, J.-Q. Rao, D. Wang, et al., "Process-Based Drying Temperature and Humidity Integration Control Enhances Drying Kinetics of Apricot Halves," *Drying Technology* 33, no. 3 (2015): 365–376, https://doi.org/10.1080/07373937.2014.954667.

53. İ. Doymaz, "Drying Kinetics, Rehydration and Colour Characteristics of Convective Hot-Air Drying of Carrot Slices," *Heat and Mass Transfer* 53 (2017): 25–35, https://doi.org/10.1007/s00231-016-1791-8.

54. R. ElGamal, C. Song, A. M. Rayan, C. Liu, S. Al-Rejaie, and G. ElMasry, "Thermal Degradation of Bioactive Compounds During Drying Process of Horticultural and Agronomic Products: A Comprehensive Overview," *Agronomy* 13, no. 6 (2023): 1580, https://doi.org/10.3390/agronomy13061580.

55. B. Akbari, N. Baghaei-Yazdi, M. Bahmaie, and F. Mahdavi Abhari, "The Role of Plant-Derived Natural Antioxidants in Reduction of Oxidative Stress," *Biofactors* 48, no. 3 (2022): 611–633, https://doi.org/10.1002/biof.1831.

56. T. Belwal, C. Cravotto, M. A. Prieto, et al., "Effects of Different Drying Techniques on the Quality and Bioactive Compounds of Plant-Based Products: A Critical Review on Current Trends," *Drying*

Technology 40, no. 8 (2022): 1539–1561, https://doi.org/10.1080/07373937.2022.2068028.

57. H. Xu, M. Wu, Y. Wang, et al., "Effect of Combined Infrared and Hot Air Drying Strategies on the Quality of *Chrysanthemum* (*Chrysanthemum morifolium* Ramat.) Cakes: Drying Behavior, Aroma Profiles and Phenolic Compounds," *Foods* 11, no. 15 (2022): 2240, https://doi.org/10.3390/foods11152240.

58. A. Antony and M. Farid, "Effect of Temperatures on Polyphenols During Extraction," *Applied Sciences* 12, no. 4 (2022): 2107, https://doi.org/10.3390/app12042107.

59. V. Shrinath, S. Gaur, K. Kaur, P. Thakur, and A. Mahajan, "Antioxidant Properties of Orange Peel and Their Implications for Health: A Comprehensive Review," *Journal of Food Chemistry and Nanotechnology* 9, no. S1 (2023): S546–S553, https://doi.org/10.17756/jfcn.2023-s1-069.

60. S. Al Hasani, Z. Al-Attabi, M. Waly, N. Al-Habsi, L. Al-Subhi, and M. Shafiur Rahman, "Polyphenol and Flavonoid Stability of Wild Blueberry (*Sideroxylon mascatense*) During Air- and Freeze-Drying and Storage Stability as a Function of Temperature," *Foods* 12, no. 4 (2023): 871, https://doi.org/10.3390/foods12040871.

61. A. Krakowska-Sieprawska, A. Kiełbasa, K. Rafińska, M. Ligor, and B. Buszewski, "Modern Methods of Pre-Treatment of Plant Material for the Extraction of Bioactive Compounds," *Molecules* 27, no. 3 (2022): 730, https://doi.org/10.3390/molecules27030730.

62. K. Jomova, R. Raptova, S. Y. Alomar, et al., "Reactive Oxygen Species, Toxicity, Oxidative Stress, and Antioxidants: Chronic Diseases and Aging," *Archives of Toxicology* 97, no. 10 (2023): 2499–2574, https://doi.org/10.1007/s00204-023-03562-9.

63. A. Czubaszek, A. Czaja, A. Sokół-Łętowska, J. Kolniak-Ostek, and A. Z. Kucharska, "Changes in Antioxidant Properties and Amounts of Bioactive Compounds During Simulated In Vitro Digestion of Wheat Bread Enriched With Plant Extracts," *Molecules* 26, no. 20 (2021): 6292, https://doi.org/10.3390/molecules26206292.

64. Y. Wu, Y. Liu, Y. Jia, et al., "Effects of Thermal Processing on Natural Antioxidants in Fruits and Vegetables," *Food Research International* 192 (2024): 114797, https://doi.org/10.1016/j.foodres.2024.114797.

65. S. Zielinska, I. Staniszewska, Z.-L. Liu, et al., "Effect of Cold Atmospheric Pressure Plasma Pretreatment on the Drying Kinetics, Physicochemical Properties and Selected Bioactive Compounds of Okra Pods Subjected to Hot Air Impingement Drying," *Drying Technology* 41, no. 15 (2023): 2405–2417, https://doi.org/10.1080/07373937.2023.2251050.

66. F. Shahidi and A. Hossain, "Importance of Insoluble-Bound Phenolics to the Antioxidant Potential Is Dictated by Source Material," *Antioxidants* 12, no. 1 (2023): 203, https://doi.org/10.3390/antiox12010203.

67. L. Neri, M. Faieta, C. Di Mattia, G. Sacchetti, D. Mastrocola, and P. Pittia, "Antioxidant Activity in Frozen Plant Foods: Effect of Cryoprotectants, Freezing Process and Frozen Storage," *Foods* 9, no. 12 (2020): 1886, https://doi.org/10.3390/foods9121886.

68. B. Koç, M. Koç, and U. Baysan, "Food Powders Bulk Properties," in *Food Powders Properties and Characterization* (2021), 1–36, https://doi.org/10.1007/978-3-030-48908-3_1.

69. J. C. Albuquerque, R. M. F. de Figueirêdo, A. J. de Melo Queiroz, et al., "Processing of Maranhão Mango Peels by Convective Drying and Freeze-Drying: Kinetic Study, Functional and Thermal Properties," *Journal of Food Measurement and Characterization* 18, no. 7 (2024): 6295–6309, https://doi.org/10.1007/s11694-024-02648-x.

70. R. Barretto, R. M. Buenavista, R. Pandiselvam, and K. Siliveru, "Influence of Milling Methods on the Flow Properties of Ivory Teff Flour," *Journal of Texture Studies* 53, no. 6 (2022): 820–833, https://doi.org/10.1111/jtxs.12630.

71. E. Juarez-Enriquez, G. I. Olivas, P. B. Zamudio-Flores, et al., "A Review on the Influence of Water on Food Powder Flowability," *Journal of Food Process Engineering* 45, no. 5 (2022): e14031, https://doi.org/10.1111/jfpe.14031.

72. S. B. Geethambika, V. S. Harthikote Veerendrasimha, A. K. Prakash, et al., "Effect of Moisture Content on Physical and Flow Properties of Milk–Millet Powders," *Journal of Food Process Engineering* 46, no. 10 (2023): e14198, https://doi.org/10.1111/jfpe.14198.

73. N. Kutlu, R. Pandiselvam, A. Kamiloglu, et al., "Impact of Ultrasonication Applications on Color Profile of Foods," *Ultrasonics Sonochemistry* 89 (2022): 106109, https://doi.org/10.1016/j.ultsonch.2022.106109.

74. N. Kalathil, N. Thirunavookarasu, K. Lakshmipathy, D. V. Chidanand, M. Radhakrishnan, and N. Baskaran, "Application of Light Based, Non-Thermal Techniques to Determine Physico-Chemical Characteristics, Pungency and Aflatoxin Levels of Dried Red Chilli Pods (*Capsicum annuum*)," *Journal of Agriculture and Food Research* 13 (2023): 100648, https://doi.org/10.1016/j.jafr.2023.100648.

75. S. Jurić, M. Jurić, Ż. Król-Kilińska, et al., "Sources, Stability, Encapsulation and Application of Natural Pigments in Foods," *Food Reviews International* 38, no. 8 (2022): 1735–1790, https://doi.org/10.1080/87559129.2020.1837862.

76. A. K. Molina, R. C. G. Corrêa, M. A. Prieto, C. Pereira, and L. Barros, "Bioactive Natural Pigments' Extraction, Isolation, and Stability in Food Applications," *Molecules* 28, no. 3 (2023): 1200, https://doi.org/10.3390/molecules28031200.

77. F. Punthi, B. Yudhistira, M. Gavahian, et al., "Optimization of Plasma Activated Water Extraction of Pleurotus Ostreatus Polysaccharides on Its Physiochemical and Biological Activity Using Response Surface Methodology," *Foods* 12, no. 23 (2023): 4347, https://doi.org/10.3390/foods12234347.

78. P. Chumsri, W. Panpipat, L.-Z. Cheong, and M. Chaijan, "Formation of Intermediate Amylose Rice Starch–Lipid Complex Assisted by Ultrasonication," *Foods* 11, no. 16 (2022): 2430, https://doi.org/10.3390/foods11162430.

79. Y. Ren, L. Huang, Y. Zhang, et al., "Application of Emulsion Gels as Fat Substitutes in Meat Products," *Foods* 11, no. 13 (2022): 1950, https://doi.org/10.3390/foods11131950.

80. A. Gomes and P. J. A. Sobral, "Plant Protein-Based Delivery Systems: An Emerging Approach for Increasing the Efficacy of Lipophilic Bioactive Compounds," *Molecules* 27, no. 1 (2021): 60, https://doi.org/10.3390/molecules27010060.

81. S. Sahraeian, A. Rashidinejad, and M. Niakousari, "Enhanced Properties of Non-Starch Polysaccharide and Protein Hydrocolloids Through Plasma Treatment: A Review," *International Journal of Biological Macromolecules* 249 (2023): 126098, https://doi.org/10.1016/j.ijbiomac.2023.126098.

82. B. Lapčíková, L. Lapčík, T. Valenta, P. Majar, and K. Ondroušková, "Effect of the Rice Flour Particle Size and Variety Type on Water Holding Capacity and Water Diffusivity in Aqueous Dispersions," *LWT* 142 (2021): 111082, https://doi.org/10.1016/j.lwt.2021.111082.

83. Y. B. Devi, P. Dhar, T. Kumari, and S. C. Deka, "Development of Functional Pasta From Pineapple Pomace With Soyflour Protein," *Food Chemistry Advances* 2 (2023): 100198, https://doi.org/10.1016/j.focha.2023.100198.

84. P. Bie, H. Pu, B. Zhang, J. Su, L. Chen, and X. Li, "Structural Characteristics and Rheological Properties of Plasma-Treated Starch," *Innovative Food Science & Emerging Technologies* 34 (2016): 196–204, https://doi.org/10.1016/j.ifset.2015.11.019.

85. H. Raza, K. Ameer, H. Ma, Q. Liang, and X. Ren, "Structural and Physicochemical Characterization of Modified Starch From Arrowhead Tuber (*Sagittaria sagittifolia* L.) Using Tri-Frequency Power Ultrasound," *Ultrasonics Sonochemistry* 80 (2021): 105826, https://doi.org/10.1016/j.ultsonch.2021.105826.

86. S. Sonkar, S. Jaddu, R. C. Pradhan, et al., "Effect of Atmospheric Cold Plasma (Pin Type) on Hydration and Structure Properties of Kodo–Millet Starch," *LWT* 182 (2023): 114889, https://doi.org/10.1016/j.lwt.2023.114889.

87. D. Nishimoto-Sauceda, L. E. Romero-Robles, and M. Antunes-Ricardo, "Biopolymer Nanoparticles: A Strategy to Enhance Stability, Bioavailability, and Biological Effects of Phenolic Compounds as Functional Ingredients," *Journal of the Science of Food and Agriculture* 102, no. 1 (2022): 41–52, https://doi.org/10.1002/jsfa.11512.

88. M. Mandal, M. Sarkar, A. Khan, et al., "Reactive Oxygen Species (ROS) and Reactive Nitrogen Species (RNS) in Plants–Maintenance of Structural Individuality and Functional Blend," *Advances in Redox Research* 5 (2022): 100039, https://doi.org/10.1016/j.arres.2022.100039.

89. K. Dome, E. Podgorbunskikh, A. Bychkov, and O. Lomovsky, "Changes in the Crystallinity Degree of Starch Having Different Types of Crystal Structure After Mechanical Pretreatment," *Polymers* 12, no. 3 (2020): 641, https://doi.org/10.3390/polym12030641.

90. P. Pękala, M. Szymańska-Chargot, and A. Zdunek, "Interactions Between Non-Cellulosic Plant Cell Wall Polysaccharides and Cellulose Emerging From Adsorption Studies," *Cellulose* 30, no. 15 (2023): 9221–9239, https://doi.org/10.1007/s10570-023-05442-y.

91. B. Zhang, Y. Gao, L. Zhang, and Y. Zhou, "The Plant Cell Wall: Biosynthesis, Construction, and Functions," *Journal of Integrative Plant Biology* 63, no. 1 (2021): 251–272, https://doi.org/10.1111/jipb.13055.

92. S. Y. Song, C. H. Kim, S. J. Im, and I.-J. Kim, "Discrimination of Citrus Fruits Using FT-IR Fingerprinting by Quantitative Prediction of Bioactive Compounds," *Food Science and Biotechnology* 27 (2018): 367–374, https://doi.org/10.1007/s10068-017-0263-3.

93. X. Li, B. Wang, W. Hu, et al., "Effect of γ-Irradiation on Structure, Physicochemical Property and Bioactivity of Soluble Dietary Fiber in Navel Orange Peel," *Food Chemistry: X* 14 (2022): 100274, https://doi.org/10.1016/j.fochx.2022.100274.

Supporting Information

Additional supporting information can be found online in the Supporting Information section.

Table S1: Model comparison of different thin layer models for control and treated PDSOPP at different flow rates and temperature. **Table S2:** Model comparison of different thin layer models for control and treated PDSOPP at different flow rates and temperature. **Table S3:** Model comparison of different thin layer models for control and treated PDSOPP at different flow rates and temperature.